




Differential gene expression reprogramming in the midgut of *Anticarsia gemmatalis* (Lepidoptera: Noctuidae) triggered by an SKTI-derivative tripeptide protease inhibitor compared to the natural SKTI protein

EULÁLIO GUTEMBERG DIAS DOS SANTOS^{1*}, NEILIER RODRIGUES DA SILVA JÚNIOR^{1*}, MARCO AURÉLIO FERREIRA³, IAN DE PAULA ALVES PINTO¹, MONIQUE DA SILVA BONJOUR¹, PEDRO MARCUS PEREIRA VIDIGAL², ELIZABETH PACHECO BATISTA FONTES¹, MARIA GORETI ALMEIDA OLIVEIRA^{1*} and HUMBERTO JOSUÉ OLIVEIRA RAMOS^{1,2*,**} 

¹ Laboratory of Enzymology and Biochemistry of Proteins and Peptides, Department of Biochemistry and Molecular Biology, Universidade Federal de Viçosa, UFV, BIOAGRO/INCT-IPP, Viçosa-MG, Brazil; e-mails: eulaliobqi@gmail.com, neilierjunior@gmail.com, ian.pinto@ufv.br, monique.bonjour@ufv.br, bbfontes@ufv.br, mgoalmeida@gmail.com, humramos@ufv.br

² Núcleo de Análise de Biomoléculas, NuBioMol, Universidade Federal de Viçosa, Viçosa-MG, Brazil; e-mail: pedro.vidigal@ufv.br

³ Laboratory of Plant Molecular Biology, Department of Biochemistry and Molecular Biology, Universidade Federal de Viçosa, UFV, BIOAGRO/INCT-IPP, Viçosa-MG, Brazil; e-mail: marco.aurelioferreira@hotmail.com

Key words. Plant defense, insect-plant interaction, transcriptome analysis, midgut, peritrophic matrix

Abstract. The velvetbean caterpillar, *Anticarsia gemmatalis*, is one of the major insect pests causing defoliation in soybean crops. Alternative strategies have been explored to reduce insect damage, including the use of protease inhibitors (PIs) that act as anti-nutritional factors. The tripeptide GORE-2, designed based on the soybean SKTI PI, exhibits enhanced protease inhibitory activity and reduces caterpillar survival. To investigate the molecular response to these PIs, we analyzed gene expression profiles using RNA-Seq. Both SKTI and GORE-2 induced extensive transcriptional reprogramming in the midgut after 24 h of exposure. The response patterns were generally similar, with changes in the expression of genes encoding digestive proteases and defense-related proteins, particularly those involved in peritrophic matrix protection and regeneration. However, SKTI elicited a more robust activation of defense signaling pathways, suggesting a stronger ability to trigger protective responses. This may explain the greater efficacy of GORE-2 in inhibiting proteolysis and reducing caterpillar survival potentially involving both amino acid starvation signaling and broader perception mechanisms developed to detect soybean-derived deterrents. As a mimetic tripeptide, GORE-2 may engage these pathways less efficiently. Notably, genes associated with detoxification and oxidative stress were more highly expressed in response to GORE-2, highlighting an additional advantage of using synthetic or mimetic protease inhibitors.

1. INTRODUCTION

Anticarsia gemmatalis Hübner (Lepidoptera: Noctuidae) is a pest insect that causes the defoliation of several crops, mainly soybean, leading to significant economic losses (Fernandes et al., 2018; Plata-Rueda et al., 2020). Chemical insecticides are a relevant tool facing this challenge and are effective against several pests, mainly caterpillars (Fernandes et al., 2018; Bel et al., 2019). However, in the larvae of *A. gemmatalis*, reduced susceptibility has been documented to older classes of synthetic insecticides, particularly organophosphates and carbamates, as well as pyrethroids, indicating a species-specific acquisition of resistance mechanisms (Boaventura et al., 2020; Lima et al.,

2024). These patterns of tolerance have driven the adoption of new chemistries: anthranilic diamides and oxadiazines to restore effective control, requiring alternatives to reduce human health toxicity and cause less environmental contamination (Campos et al., 2019; Boaventura et al., 2020).

New strategies to mitigate pest damage have focused on the development of bioinsecticides, which show great potential due to their ability to limit caterpillar development while exhibiting lower toxicity compared to conventional chemical insecticides (Meriño-Cabrera et al., 2018; da Silva Júnior et al., 2020). Notable examples of bioinsecticides include *Bacillus thuringiensis* (Bt) toxins derived

* These authors contributed equally to this work.

** Corresponding author; e-mail: humramos@ufv.br

from microbial sources (Pezenti et al., 2021) and protease inhibitors (PIs).

PIs are proteins or peptides with insecticidal activity that can be naturally produced by plants or synthesized chemically. They represent one of the most abundant classes of natural defenses used by plants against insect herbivory (Zhao et al., 2019). A well-known example is the Soybean Kunitz Trypsin Inhibitor (SKTI). The expression of PIs in soybean is induced by mechanical damage caused by the chewing action of phytophagous insects (Kuwar et al., 2015; Meriño-Cabrera et al., 2022). These mechanical stimuli activate plant defense signaling pathways, notably the lipoxygenase cascade (Mahanta et al., 2025), leading to increased synthesis of PIs. Once ingested, SKTI inhibits specific catalytic sites of midgut digestive enzymes, decreasing the availability of essential amino acids that are crucial for insect growth and physiological functions (Kuwar et al., 2015; Mendonça et al., 2020).

However, large-scale field application of PI-based bioinsecticides remains challenging due to their inherent instability under environmental conditions, short shelf-life, and high production costs, which collectively hinder their widespread adoption in agriculture (Qu et al., 2022). Furthermore, the co-evolutionary dynamics of plant-insect interactions have driven insects to develop adaptive responses to PI exposure. Insects such as caterpillars respond by upregulating protease expression (Shakeel & Zafar, 2020) and synthesizing new enzyme isoforms that evade inhibition (Coura et al., 2022). These strategies enable insects to compensate for nutrient limitations and maintain digestive efficiency, thus demonstrating a degree of physiological plasticity in adapting to plant defenses (Coura et al., 2022; Silva-Júnior et al., 2021).

Previous studies investigating the action of protease inhibitors (PIs) in lepidopteran larvae have primarily focused on the midgut, which is the main site of protein digestion due to its high serine protease activity. These enzymes accounting for approximately 95% of total digestive proteolytic activity (Ponnuvel et al., 2015; Taprok et al., 2015; Silva-Júnior et al., 2021). These studies have demonstrated that PIs can inhibit key digestive enzymes such as trypsins and chymotrypsins, leading to compensatory overexpression of protease isoforms and altered expression of genes associated with nutrient absorption and detoxification (Visotto et al., 2009; Terra & Ferreira, 2012; Roy et al., 2022).

In addition to digestive modulation, other research has highlighted immune-related responses triggered by PIs. For example, increased expression of oxidoreductase enzymes, including catalases and peroxidases, has been reported, which contribute to the protection of midgut epithelial structures such as the peritrophic matrix, chitin layer, and mucin-like proteins (Li et al., 2009; Toprak et al., 2010; Wang et al., 2022). These changes are part of a broader physiological adaptation to cope with PI-induced stress.

Despite these advances, most of the current knowledge is based on studies using full-length natural plant PIs. There

remains limited understanding of how small PI-derived peptides, such as synthetic tripeptides mimicking active motifs and affect gene expression in *A. gemmatilis*, particularly at a genome-wide scale. Therefore, our study aims to address this gap by comparing the transcriptomic responses of *A. gemmatilis* larvae exposed to a SKTI-derived tripeptide inhibitor versus the native SKTI protein, revealing novel insights into midgut reprogramming and potential biotechnological targets for pest control.

Previous research conducted by our group has focused on the rational design of smaller and more stable synthetic peptides derived from plant protease inhibitors, aiming to preserve inhibitory potential while reducing the activation of immune defenses in target insects. One such compound is the tripeptide GORE-2 (Val-Leu-Arg), designed based on the active motif of the soybean Kunitz trypsin inhibitor (SKTI). *In vitro* and *in vivo* assays demonstrated that GORE-2 binds with high affinity to trypsin-like catalytic sites and functions as a competitive inhibitor of serine proteases, significantly impairing digestive physiology in *A. gemmatilis*. Molecular docking simulations revealed that GORE-2 forms stable hydrogen bonds with key active site residues of *A. gemmatilis* trypsin-like enzymes, indicating effective inhibition. Furthermore, *in vivo* studies showed that larvae fed with GORE-2 exhibited higher mortality rates and reduced pupal weights compared to those treated with SKTI, highlighting the enhanced efficacy of this synthetic peptide.

These findings underscore the potential of GORE-2 as a promising tool in the management of *A. gemmatilis*, offering advantages over natural inhibitors by inducing significant physiological disruptions in the pest's midgut. To better understand the physiological and molecular responses elicited by this synthetic inhibitor in comparison to the native SKTI protein, we performed transcriptome sequencing of *A. gemmatilis* larvae exposed to each compound. This strategy enabled us to identify distinct gene expression patterns and enriched pathways associated with digestion, metabolism, and immune modulation. These findings demonstrated that synthetic inhibitor GORE-2 peptide and Kunitz-type inhibitors can differentially modulate larval proteolytic activity and compromise pest development through gut-specific effects (Barros et al., 2022; Meriño-Cabrera et al., 2022).

2. MATERIAL AND METHODS

2.1. *Anticarsia gemmatilis* caterpillars

Anticarsia gemmatilis eggs were maintained at $25 \pm 2^\circ\text{C}$ and $70 \pm 10\%$ relative humidity in the Insect Laboratory of the Department of Biochemistry and Molecular Biology at the Federal University of Viçosa (UFV). The average biological cycle of the soybean caterpillar is four to five weeks. Adults were housed in 50×50 cm screened cages, internally lined with A4 bond paper sheets. Pupae were placed in 150×20 mm Petri dishes inside the cages until adult emergence.

Adult moths were fed with a nutrient solution containing honey (20.0 g), beer (350 mL), sucrose (50 g), ascorbic acid (1.05 g), nipagin (1.05 g), and distilled water (650 mL). The solution was absorbed onto a cotton swab positioned in a Petri dish at the bot-

tom of each cage. After oviposition, paper sheets containing the eggs were cut into strips (2.5×10 cm) and transferred to 500 mL plastic containers with a circular opening (approximately 2 cm in diameter) in the lid, which was covered with organza fabric. These containers were maintained in a climate-controlled chamber at 25°C , $60 \pm 10\%$ relative humidity, and a 14 h photoperiod. Upon hatching, the larvae were fed an artificial diet, with a cube of diet placed into each container.

2.2. Preparation of the artificial diet and treatments

The artificial diet consisted of cooked Mulato beans, brewer's yeast, wheat germ, soy protein, casein, agar, and water. Agar and water were autoclaved for 20 min at 1.5 kgF cm^{-2} pressure, and the ingredients were mixed in an industrial blender. Then ascorbic acid (6.0 g), nipagin (methylparaben) (5.0 g), 40% formaldehyde (6.0 mL), and 23 mL of a vitamin solution composed of niacinamide (1.0 mg), calcium pantothenate (1.0 mg), thiamine (0.25 mg), riboflavin (0.5 mg), pyridoxine (0.25 mg), folic acid (0.25 mg), biotin (0.02 mg), inositol (20 mg) and water (1.0 L) to form a homogeneous paste, transferred while still hot to plastic containers with lids. The control group was fed a diet without protease inhibitors, and the other two groups were fed a diet with protease inhibitors GORE-2 or SKTI. The fifth instar larvae were maintained in cages 3×5 cm and fed ad libitum on a diet (control) and diets supplemented with sublethal PIs concentration: 0.12% (w/w) of serine-protease Kunitz (SKTI) (treatment 1) and 0.12% (w/w) of GORE-2 (treatment 2), as described by Chougule et al. (2008). After 24 h, the caterpillars were collected from each treatment and control. The diets cooled in a germicidal chamber under ultraviolet light were kept at 4°C before being administered to the caterpillars. The caterpillars were immobilized on ice, and the midgut was carefully dissected under a stereomicroscope by making a longitudinal incision along the dorsal side of the body. The intestines were gently removed, rinsed in cold sterile saline to eliminate gut contents, and immediately transferred to RNase-free microtubes. The tissue was snap-frozen in liquid nitrogen and stored at -80°C until total RNA extraction for transcriptome analysis via RNA sequencing (RNA-Seq).

2.3. RNA extraction and transcriptome sequencing

In our experimental design, three independent biological replicates were performed for each treatment group (Control, SKTI, and GORE-2), yielding nine midgut samples. Total RNA was extracted from each replicate using TRIzol reagent (Invitrogen) following the manufacturer's protocol. Three units of DNase, free of RNase (Invitrogen), treat the extracted RNA to eliminate contamination by DNA. RNA was quantified in a NanoDrop spectrophotometer (Thermo Scientific) at 260/280 nm and analyzed with a 1.5% (w/v) denaturing agarose gel, stained with $0.1 \mu\text{g mL}^{-1}$ ethidium bromide. The construction of individual cDNA libraries used the Illumina® TruSeq Stranded mRNA Kit according to the instructions provided by the manufacturer. Sequencing was performed on the Illumina® HiSeq 2500 by the Beijing Genomics Institute (BGI), producing paired-end reads of 100 nucleotides.

2.4. Quality analysis and assembly

The quality control of raw sequencing data was performed using FastQC version 0.11.7 (Andrews, 2010), combined using MultiQC version 1.12 (Ewels et al., 2016). Sequences' adapters removal used the "auto-detection" setting of TrimGalore version 0.6.7 (Krueger, 2021). Then, the reads were trimmed for quality and filtered for length using the Trimmomatic version 0.39 (Bolger et al., 2014) with the following parameters: HEADCROP: 15; LEADING: 3; TRAILING: 3; SLIDINGWINDOW: 4:20; MINLEN: 50. Trimmed sequences were additionally processed by Rcorrector version 1.0.4 (Song & Florea, 2015), using the de-

fault settings and applying a sequence correction method based on k-mers sequences analysis.

The transcriptome was assembled de novo using Trinity version 2.8.5 (Grabherr et al., 2011), selecting the default settings and filtering the transcripts to a minimum length of 500 nucleotides. The script "TrinityStats.pl" calculated descriptive statistics of the assembly. The transcriptome was also evaluated by mapping the reads to the transcript sequences using Bowtie2 tools version 2.2.6 (Langmead et al., 2012), selecting default settings "--end-to-end" and "--sensitive". After assembly, the CD-hit-est tool of CD-HIT version 4.8.1 (Fu et al., 2012) clustered the transcripts into non-redundant Unigene sequences, selecting a minimum global identity of 98%.

2.5. ORF prediction

Open reading frames (ORFs) were predicted from the assembled unigene sequences using TransDecoder.LongOrfs (v5.5.0), a widely used tool for identifying candidate coding regions within de novo transcriptome assemblies (Haas et al., 2013). Only ORFs with a minimum length of 300 nucleotides were retained for downstream analyses. TransDecoder.LongOrfs was selected due to its robustness in detecting biologically relevant coding regions in non-model organisms without reference genomes. The protein sequences encoded by the predicted ORFs were compared with proteins available in the UniProt Knowledgebase database (UniProtKB, <http://www.uniprot.org/>) (UniProt Consortium, 2014) using the BLASTp tool of BLAST version 2.11.0 (Altschul et al., 1990). Protein sequences were also identified with the support of Hidden Markov Models (HMMs) of domain families from the Pfam database (<http://pfam.xfam.org/>) (Finn et al., 2014) using HMMER version 3.1b2 (Eddy & Wheeler, 2015). Only alignments that showed an E-value score $\leq 1 \times 10^{-10}$ were considered significant. The BLASTp alignments were also evaluated for sequence similarity, selecting those showing the product coverage \times similarity $\geq 40\%$. The TransDecoder.predict tool predicted the proteins encoded by the Unigenes by consolidating the results of ORF prediction with the results of similarity searches using BLASTp and HMMER.

2.6. Differentially expressed transcript analysis

The transcript abundance was quantified by Kallisto version 0.44.0 (Bray et al., 2016), performing a pseudo-alignment of the reads against the Unigenes sequences. Differential expression analysis was performed using DESeq2 v3.15 (Love et al., 2014) on three independent biological and technical replicates per condition. Genes were considered significantly differentially expressed if they exhibited a Benjamini-Hochberg adjusted p-value < 0.05 and an absolute \log_2 fold change ≥ 1 ($|\text{FC}| \geq 2$). The contrasts analyzed were GORE-2 vs. control, SKTI vs. control, and GORE-2 vs. SKTI.

2.7. Functional annotation

Functional annotation of the unigene sequences was performed using TRAPID version 2.0 (Van Bel et al., 2013), with the eggNOG database version 4.5.1 (Huerta-Cepas et al., 2016, 2017) as the reference. An E-value threshold of $\leq 1 \times 10^{-10}$ was applied for gene family assignment, identification of functional domains, and Gene Ontology (GO) term annotation.

Differentially expressed unigenes were further annotated using BLAST2GO (Conesa et al., 2005), based on automatic sequence alignment against Arthropoda protein entries (NCBI Taxonomy ID: 6656) available in the NCBI RefSeq non-redundant (nr) protein database. Alignments with E-values $\leq 1 \times 10^{-10}$ were considered significant.

Metabolic pathway enrichment analysis of the differentially expressed unigenes was conducted using KOBAS (Xie et al.,

2011), applying the hypergeometric statistical test with an adjusted *p*-value cutoff of < 0.05 . Genome annotations of *Helicoverpa armigera* and *Bombyx mori* were used as references for KEGG orthology assignment.

2.8. Statistical analysis of RNA-Seq data

Statistical analysis of differential expression was conducted using the *DESeq2* package (Love et al., 2014) in the R environment. For each pairwise comparison (Control vs SKTI, Control vs GORE-2, and SKTI vs GORE-2), genes with a false discovery rate (FDR) < 0.05 and absolute \log_2 fold change ($|\log_2FC|$) ≥ 1 were considered significantly differentially expressed. *P*-values were adjusted for multiple testing using the Benjamini-Hochberg procedure. Principal component analysis (PCA) was performed using *DESeq2* to assess sample clustering and variation between treatments. Volcano plots and heatmaps were generated with the *ggplot2* and *pheatmap* packages, respectively, to visualize the distribution and intensity of differentially expressed genes.

Gene Ontology (GO) and KEGG pathway enrichment analyses were performed using the KOBAS package (Xie et al., 2011), applying hypergeometric testing and adjusting *p*-values using FDR correction. Enriched categories were considered significant at an adjusted *p*-value < 0.05 .

3. RESULTS

3.1. Data analysis sequencing

The sequencing of *A. gemmatalis* midgut libraries yielded between 46 and 48 million raw reads per sample, each comprising 100 nucleotides, with an average GC content of 48%. Post adapter removal and quality trimming, the datasets retained approximately 43 to 44 million high-quality reads, ranging from 50 to 85 nucleotides in length. These metrics align with established standards for RNA-Seq experiments, where a sequencing depth of 30 to 60 million reads per sample is considered adequate for comprehensive transcriptome analysis, and a GC content around 50% is typical for insect genomes. Furthermore, the read length distribution post-trimming falls within the acceptable range for downstream analyses, ensuring reliable gene expression quantification.

3.2. Reference transcriptome assembly

The reference transcriptome assembly identified 51,825 transcripts. The mean length of the transcripts obtained was 2,243.6 nt, and the N50 was 3,246 nt (Table S1). The validation of transcriptome by reads mapping showed that 86% of aligned reads in the transcripts and 14.31% did not align. Furthermore, 20.33% of aligned uniquely, and 65.36% had multiple alignments. The sequences of transcripts were grouped in 42,372 Unigenes, which have an average of 1,467 nt in size and an N50 of 2,894 nt.

3.3. Functional annotation

A total of 42,372 open reading frames (ORFs) were predicted from the assembled *A. gemmatalis* unigenes. Among the encoded proteins, 25,906 (50.01%) showed significant similarity to known proteins in the UniProt database (Fig. S1). Taxonomic profiling of these aligned sequences revealed that 36% matched proteins from *Bombyx mori*, 34% from *Danaus plexippus*, 25% from *Heliconius melpomene*, and the remaining 5% from other insect taxa, indicating

a strong correspondence with available Lepidopteran reference proteomes. The same pattern was reflected in the eggNOG database, where protein sequences from *B. mori* and *D. plexippus* accounted for 70% of significant hits, reinforcing the phylogenetic relevance of these species to *A. gemmatalis*.

Functional annotation resulted in 22,040 significant matches in the Swiss-Prot database and 20,762 entries associated with orthologous groups in eggNOG. Moreover, 13,731 Gene Ontology (GO) terms were assigned to the dataset, and 13,223 unigenes were classified into KEGG Orthology (KO) groups. Notably, the KO1312 orthologous group, corresponding to trypsin-like serine proteases, was the most represented, with 145 entries, reflecting the dominance of serine protease activity in Lepidopteran midgut physiology. Searches in the *Pfam* database further identified 32,673 conserved protein domains across the predicted ORFs, supporting the diversity of functional elements in the midgut transcriptome. Together, these results provide robust multi-database coverage and high-quality annotation, consistent with standards observed in non-model insect transcriptomics.

The functional categorization of unigenes expressed in the *A. gemmatalis* midgut transcriptome revealed a predominance of genes associated with digestion, immunity, and detoxification (Fig. 1). The most abundant gene family was trypsin, with 145 annotated entries classified under the PRS1_2_3 group, supporting its central role in protein digestion. Serpin B, a major family of serine protease inhibitors involved in immune modulation, was represented by 82 unigenes, while cytochrome P450s were predominantly from families CYP6 (88 entries) and CYP9 (56 entries). Additional enzyme classes included UDP-glucuronosyltransferases (90 unigenes), glutathione S-transferases (45), and β -glucosidases (36), all of which are involved in xenobiotic metabolism and secondary metabolite processing. The presence of 46 MFS (major facilitator superfamily) transporters and 38 LITAF-like protein entries further highlights the functional diversity related to transport and stress responses in the insect midgut.

From a COG (Clusters of Orthologous Groups) perspective (Fig. 1A), the most represented functional categories were amino acid transport and metabolism (173 unigenes), lipid metabolism (99), protein folding and modification (86), carbohydrate metabolism (86), and defense mechanisms (71). These results are consistent with the midgut's physiological role as a hub for digestion and immune surveillance. Furthermore, the unigene annotations revealed high expression of proteolytic enzymes (Fig. 1B), such as trypsins (145), serine endopeptidases (68), and lipases (68), indicating robust digestive activity. The high frequency of immune-related genes, particularly serpins, also underscores the midgut's function in regulating proteolytic cascades and responding to biotic stress (Fig. 1C).

The expression of genes encoding detoxification enzymes, such as cytochrome P450s, UDP-glucuronosyltransferases, and glutathione S-transferases, suggests a midgut-mediated response to xenobiotics, likely triggered

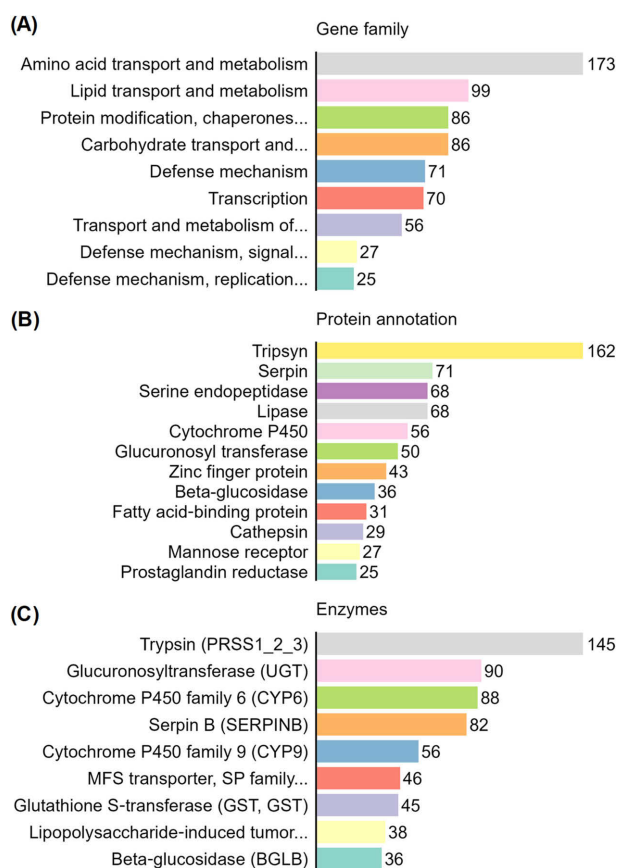


Fig. 1. Functional categorization of midgut transcriptome unigenes from *A. gemmatilis*. (A) Distribution of unigenes across major COG functional categories, highlighting genes involved in amino acid transport and metabolism (173), lipid metabolism (99), protein folding and modification (86), carbohydrate metabolism (86), defense mechanisms (71), and transcriptional regulation (70). (B) Most frequent protein annotations include trypsin (162), serpin (71), serine endopeptidase (68), lipase (68), cytochrome P450 (56), UDP-glucuronosyltransferase (50), zinc-finger protein (43), β -glucosidase (36), fatty acid-binding protein (31), cathepsin (29), mannose receptor (27), and prostaglandin reductase (25). (C) Enzyme family distribution reveals dominance of trypsins (PRSS1_2_3; 145), UDP-glucuronosyltransferases (UGT; 90), cytochrome P450 family 6 (CYP6; 88) and family 9 (CYP9; 56), serpin B (82), MFS transporters (46), glutathione S-transferases (GST; 45), LITAF-like proteins (38), and β -glucosidases (36). Bars represent the number of unigenes annotated for each category, underscoring the physiological importance of digestion, immunity, and detoxification in the larval midgut.

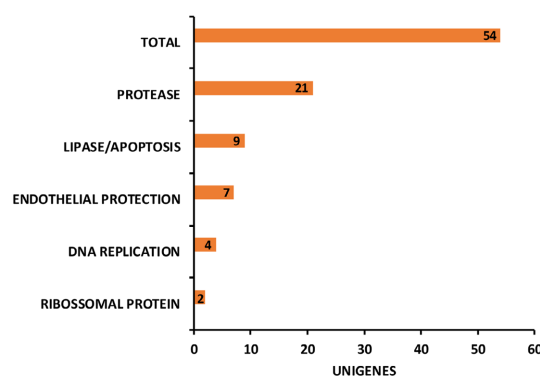


Fig. 2. Description of annotated unigenes with the highest normalized average expression levels, measured in transcripts per million (TPM). Expression values were obtained using the Kallisto and DESeq2 pipeline, highlighting the response of *A. gemmatilis* midgut to treatments with the protease inhibitors GORE-2 and SKTI.

by dietary exposure to plant allelochemicals. Notably, GSTs exhibit peroxidase activity and, along with ascorbate peroxidases (APOX), contribute to peroxide detoxification in insect gut tissues (Wang et al., 2022). The detection of 36 β -glucosidase entries further supports a role in both digestion of glycosylated compounds and defense-related hydrolysis of plant secondary metabolites.

3.4. GORE-2 and SKTI inhibitors alter mainly the protease expression

The average transcript counts per million (TPM) observed in treatments with GORE-2 and SKTI were used to assess the impact of these protease inhibitors (PIs) on the midgut transcriptome of *A. gemmatilis* larvae. The 50 unigenes with the highest mean TPM values and UniProt-based annotations were selected for further analysis (Fig. 2). Among these, both PIs induced the expression of 21 unigenes encoding proteolytic enzymes with extracellular digestive functions, including trypsins, serine proteases, chymotrypsins, and collagenases. Additionally, 9 unigenes were annotated as lipases, linked to lipid degradation and apoptosis pathways; 7 were associated with structural roles; and 4 were related to DNA replication activity.

As anticipated, the most frequently induced transcripts corresponded to proteases. Notably, changes were also observed in the expression of genes associated with apoptosis and epithelial protection (Fig. 2 and Table 1). In addition

Table 1. Differentially expressed genes associated with peritrophic matrix protection in *Anticarsia gemmatilis* larvae fed with protease inhibitors (GORE-2 or SKTI) compared to the control.

TARGET_ID	TPM AVERAGE SKTI	TPM AVERAGE GORE-2	TPM AVERAGE SKTI/GORE-2	FUNCTION
TRINITY_DN360_c0_g3_i4	5965,37	11767,86667	8866,62	Putative cuticle protein CPH45
TRINITY_DN360_c0_g3_i2	1202,852667	2084,717333	1643,79	Putative cuticle protein CPH45
TRINITY_DN2772_c0_g1_i5	2064,003333	2478,556333	2271,28	Peritrophin type-A domain protein 2
TRINITY_DN2843_c0_g1_i1	1824,379333	1423,568	1623,97	Insect intestinal mucin
TRINITY_DN4963_c0_g2_i1	1530,629	1330,46	1430,54	Glutathione S-transferase 1-like isoform X1
TRINITY_DN3649_c0_g1_i3	2493,056667	1622,8464	2057,95	Glutaredoxin
TRINITY_DN840_c0_g3_i1	5209,747333	795,9056667	3002,83	Chitin-binding protein
TRINITY_DN2469_c0_g1_i1	3650,155	702,9383333	2176,55	Chitin deacetylase 1

TPM – Transcripts Per Kilobase Million

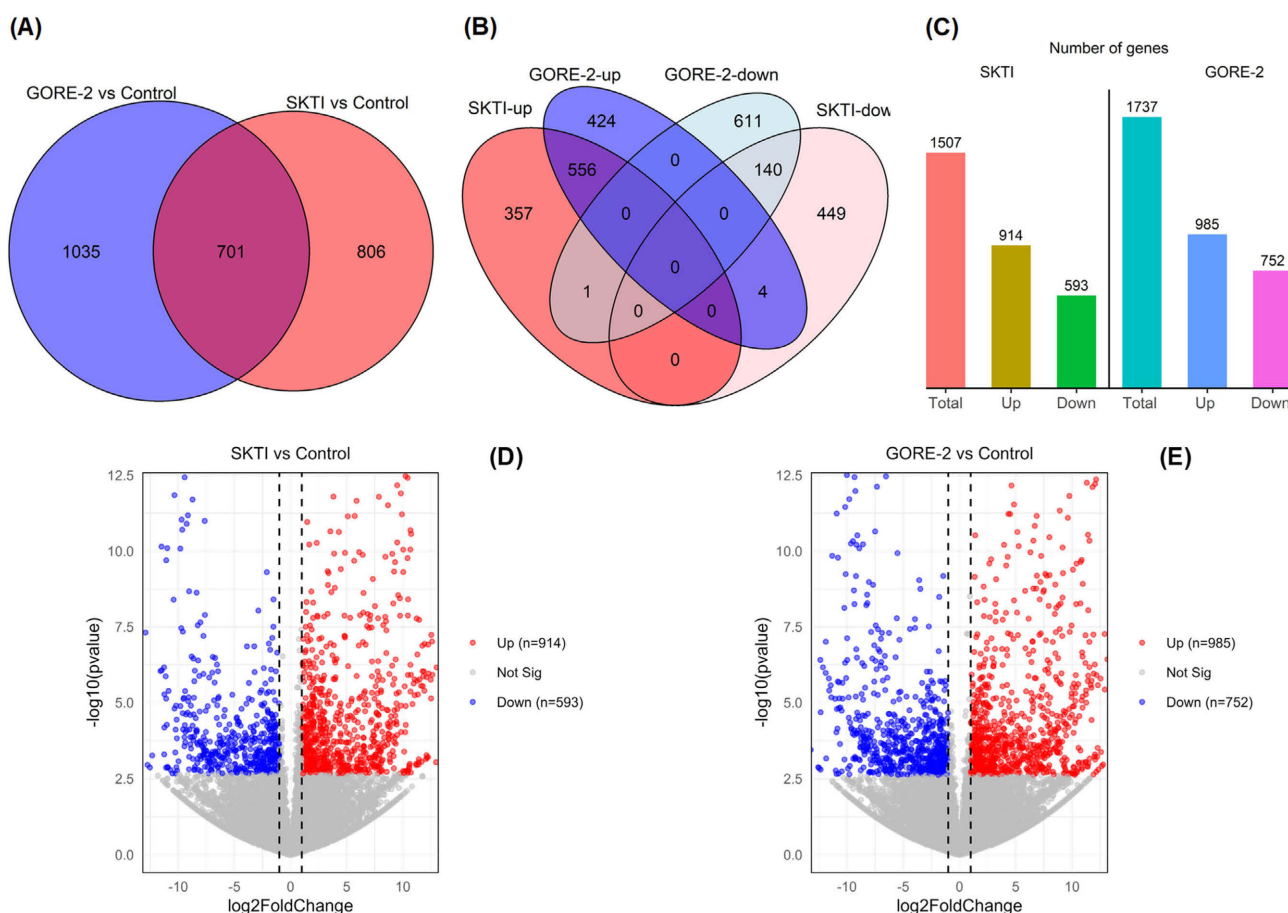


Fig. 3. Overview of differentially expressed genes (DEGs) in the midgut of *Anticarsia gemmatalis* larvae following exposure to the natural serine protease inhibitor SKTI and the synthetic tripeptide GORE-2. (A) Venn diagram showing the total number of DEGs ($FDR < 0.05$, $|\log_2 FC| \geq 1$) uniquely identified in comparisons between Control vs SKTI (light red), Control vs GORE-2 (blue), and those shared between both treatments. (B) DEG subsets categorized as up-regulated (SKTI-UP: red; GORE-2-UP: green) or down-regulated (SKTI-DW: blue; GORE-2-DW: yellow), highlighting the distinct transcriptional responses elicited by each inhibitor. (C) Bar chart summarizing the number of DEGs per category, revealing a greater number of induced transcripts under SKTI treatment and a stronger transcriptional repression associated with GORE-2. (D, E) Volcano plots of Control vs SKTI (D) and Control vs GORE-2 (E), depicting the distribution of gene expression changes: \log_2 fold-change on the x-axis and $-\log_{10}$ adjusted p-value on the y-axis. Red dots represent significantly up-regulated genes, blue dots indicate significantly down-regulated genes, and grey dots correspond to non-significant changes.

to impairing protein digestion and modulating protease expression, PIs can exert broader effects on midgut physiology. Several genes exhibited markedly elevated expression levels in PI-treated larvae compared to controls, with expression values quantified in TPM (Table 1). Genes involved in oxidative stress responses were strongly induced by both PI treatments, including glutathione S-transferase 1-like isoform X1 and glutaredoxin. Glutaredoxins and thioredoxin peroxidases are key antioxidant enzyme families that regulate cellular redox homeostasis and protect against oxidative damage. Similarly, the presence of protease inhibitors in the caterpillar diet affected the integrity of the peritrophic matrix, as evidenced by the upregulation of genes associated with intestinal defense mechanisms (Table 2). Exposure to environmental stressors promotes increased deposition of cuticular components, enhancing the insect's ability to adapt to novel or fluctuating conditions (Zhang et al., 2008). Overall, gene upregulation was more pronounced in response to SKTI than to GORE-2.

3.5. Differentially expressed transcripts were distinct for PIs SKTI and GORE-2

The comparison between SKTI and control identified 1,507 differentially expressed unigenes (DEGs), including 914 up-regulated and 593 down-regulated transcripts (Fig. 3C). Transcriptomic reprogramming was even more pronounced following treatment with the synthetic tripeptide GORE-2 than with the native soybean protease inhibitor SKTI. The comparison between GORE-2 and control revealed 1,736 DEGs, with 985 up-regulated and 752 down-regulated (Fig. 3C).

Although a comparable number of genes were differentially expressed in response to both protease inhibitors, most DEGs were specific to each treatment (Fig. 3A and B). This indicates that the molecular signaling cascades triggered by SKTI and GORE-2 were largely distinct, despite both compounds targeting proteolytic activity. These results suggest that gene expression reprogramming in the midgut is not solely governed by protease inhibition or

Table 2. Genes overexpressed in protecting *A. gemmatilis* peritrophic matrix when fed with protease inhibitors (GORE-2 or SKTI) compared to the control.

TARGET_ID	TPM AVERAGE SKTI	TPM AVERAGE GORE-2	TPM AVERAGE SKTI/GORE-2	FUNCTION
TRINITY_DN360_c0_g3_i4	5965.37	11767.87	8566.62	Putative cuticle protein CPH45
TRINITY_DN360_c0_g3_i2	1200.85	2084.71	1643.79	Putative cuticle protein CPH45
TRINITY_DN2772_c0_g1_i5	2064.01	2478.56	2271.28	Peritrophin type-A domain protein 2
TRINITY_DN2843_c0_g1_i1	1824.37	1423.56	1623.97	Insect intestinal mucin
TRINITY_DN4963_c0_g2_i1	1530.62	1330.46	1430.54	Glutathione S-transferase 1-like isoform X1
TRINITY_DN3649_c0_g1_i3	2493.05	1622.84	2057.95	Glutaredoxin
TRINITY_DN840_c0_g3_i1	5209.74	795.91	3002.83	Chitin-binding protein
TRINITY_DN2469_c0_g1_i1	3650.15	702.98	2176.55	Chitin deacetylase 1

TPM = Transcript per Kilobase Million

amino acid deprivation, but also reflects compound-specific modulation of broader physiological pathways.

3.6. Transcriptomic responses induced by SKTI and GORE-2

The DEG subsets were further classified according to the direction of expression changes (Fig. 3B). SKTI treatment resulted in a lower number of up-regulated genes, whereas GORE-2 treatment induced a more pronounced down-regulation. This trend was confirmed by the bar chart in Fig. 3C, which quantifies the DEG distribution per category. Volcano plots (Fig. 3D and 3E) illustrate the magnitude and statistical significance of the expression changes for each treatment, with a clear shift in expression dynamics indicating stronger transcriptional repression under GORE-2 exposure.

To further explore gene-level responses, the 20 most significant DEGs based on adjusted p-values and fold-change values ($FDR < 0.05$; $|\log_2 FC| \geq 1$) were visualized in a heatmap (Fig. S2 and Table S2 and S3). The heatmap depicts \log_2 fold-change values normalized across samples, with red representing up-regulation and blue indicating down-regulation relative to controls. Panels A and B correspond to SKTI and GORE-2 treatments, respectively, revealing inhibitor-specific expression signatures. Complete-linkage hierarchical clustering grouped genes by expression similarity and confirmed consistent patterns between the two biological replicates. Notably, the DEGs with the highest fold-change values (either positive or negative) were highlighted to facilitate interpretation of the most strongly affected transcripts. These results underscore the distinct transcriptional reprogramming patterns induced by the two protease inhibitors and point to specific sets of genes that may contribute to their differential physiological effects.

In the GORE-2 × Control comparison, the most frequent GOs (Fig. 4A) among the down-regulated unigenes were related to hydrolase activity (GO:0016787, 31); catalytic activity – protease (GO:0140096, 21); transmembrane transport (GO:0055085, 19); transport activity (GO:0005215, 18); oxidoreductase activity (GO:0016491, 17); transferase (GO:0016740, 16); protein modifying process (GO:0036211, 12); and lipid metabolism process (GO:0006629, 11). In the GORE-2 × Control comparison, the most frequent GOs among the up-regulated DEGs (Fig. 4C) are related to hydrolase activity (GO:0016787,

27); transmembrane transport (GO:0055085, 25); transport activity (GO:0005215, 20); transferase (GO:0016740, 20); oxidoreductase activity (GO:0016491, 20); membrane component (GO:0016020, 14); transcriptional regulation (GO:0005634, 14); and catalytic activity – protease (GO:0140096, 13).

For SKTI Down-regulated (Fig. 4B), the GOs most frequent among the down-regulated unigenes were related to hydrolase activity (GO:0016787, 15); oxidoreductase activity (GO:0016491, 11); transport activity (GO:0005215, 10); transferase (GO:0016740, 10); transmembrane transport (GO:0055085, 10); transcriptional regulation (GO:0005634, 9); membrane component (GO:0016020, 8); and catalytic activity – protease (GO:0140096, 8). The analysis of SKTI × Control, the most frequent GOs among the up-regulated unigenes (Fig. 4D) were related to hydrolase activity (GO:0016787, 26); catalytic activity (GO:0140096, 23); transferase (GO:0016740, 15); membrane component (GO:0016020, 15); oxidoreductase activity (GO:0016491, with 12); peptidase (EC 3.4) with 10; protease (EC 3.4.21) with 10; and structural molecular activity (GO:0005198) with 7.

As shown in Fig. 4, the profiles of dysregulated genes in response to the protease inhibitors were notably distinct. Within the GO category “catalytic activity – protease,” the number of down-regulated genes was 2.6 times higher under GORE-2 treatment. Conversely, SKTI treatment resulted in 1.7 times more up-regulated genes in this category. These results suggest that GORE-2 induces a weaker activation of protease gene expression in the caterpillar midgut. Similarly, genes involved in oxidative stress responses were more strongly up-regulated in the presence of GORE-2, showing a 1.7-fold increase compared to SKTI. Asterisks beside the bars in Fig. 4 highlight GO terms uniquely enriched in each contrast. SKTI treatment specifically down-regulated eight contigs related to transcriptional regulation, whereas GORE-2 selectively up-regulated fourteen contigs in this same category. These findings provide additional evidence that SKTI and GORE-2 activate distinct regulatory cascades. Similarly, seventeen contigs annotated as peptidases were exclusively up-regulated in the SKTI-treated group. Moreover, comparison of GO terms between SKTI-UP and GORE-2-UP categories revealed that contigs associated with RNA binding, splicing,

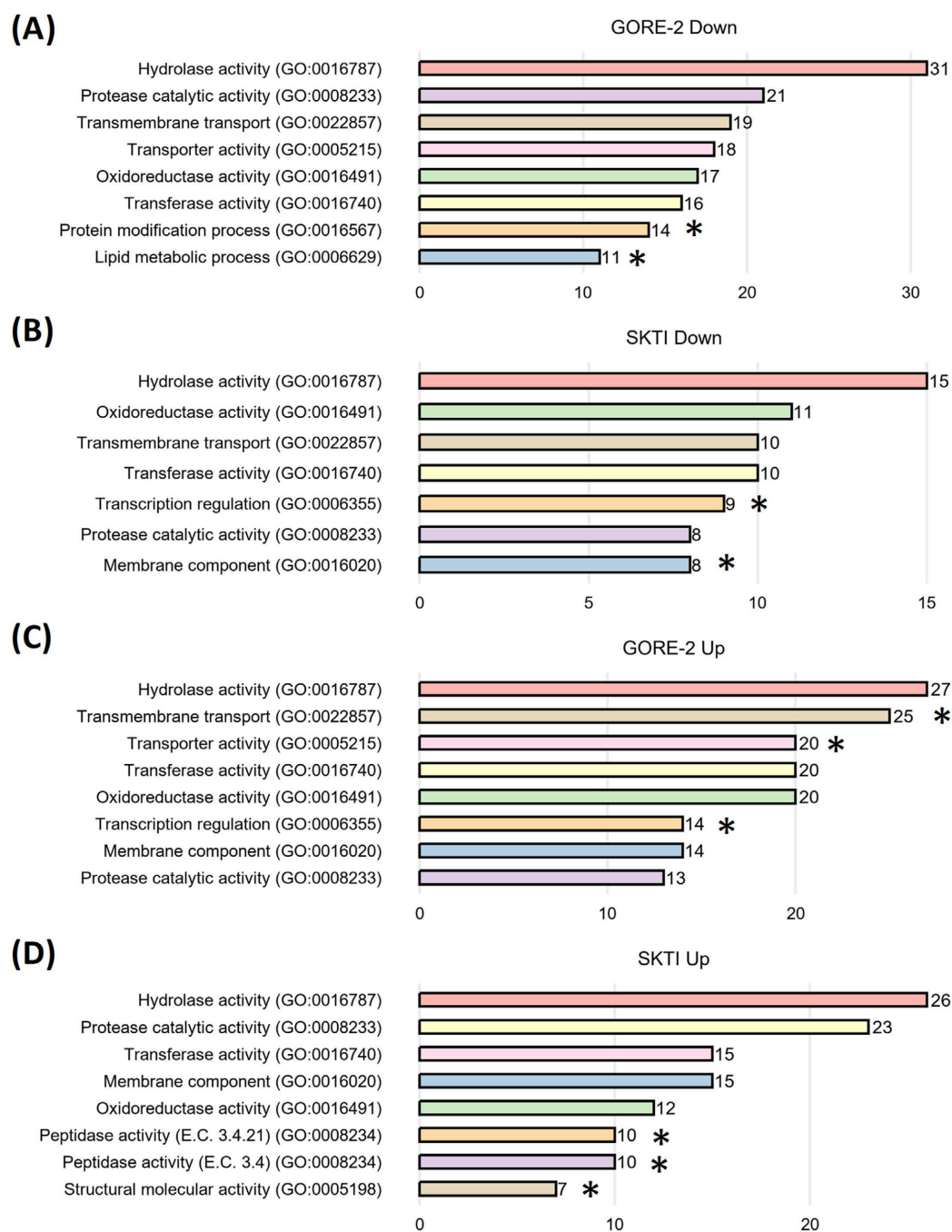


Fig. 4. Enrichment of Gene Ontology (GO) categories among differentially expressed midgut unigenes of *Anticarsia gemmatilis* following treatment with the synthetic protease inhibitor GORE-2 and the natural inhibitor SKTI. Horizontal bar-chart panels display the eight most abundant GO biological-process terms in down-regulated (A, B) and up-regulated (C, D) gene sets for Control vs GORE-2 (A, C) and Control vs SKTI (B, D) comparisons (FDR < 0.05, $|\log_2 FC| \geq 1$). Bars are colored by GO term using the Pastel1 palette, with black outlines on a white background; raw unigene counts are printed at the distal end of each bar. GO terms are shown in full on the y-axis, each followed by its accession ID in parentheses (e.g., Hydrolase activity (GO:0016787)). Panel A highlights biological processes most depleted by GORE-2; panel B shows those most depleted by SKTI; panel C shows the most induced by GORE-2; and panel D shows the processes most induced by SKTI. All GO annotations were assigned via the TrapID/eggNOG-mapper pipeline, and the narrower bar widths emphasize relative abundance differences across treatments.

and proteasome-related processes were found only in the GORE-2 contrast.

The KEGG pathway enrichment analysis of differentially expressed midgut genes revealed marked differences in the metabolic responses of *A. gemmatilis* larvae to the natural inhibitor SKTI and the synthetic inhibitor GORE-2. As illustrated in Fig. 5, the top ten up- and down-regulated

pathways for each treatment were evaluated based on enrichment ratios (DEGs ÷ total annotated unigenes), offering insight into functionally relevant shifts in gene expression.

In the GORE-2 vs. Control comparison (Fig. 5B), enriched pathways among up-regulated genes included those involved in xenobiotic metabolism, particularly drug metabolism by cytochrome P450, glutathione metabolism,

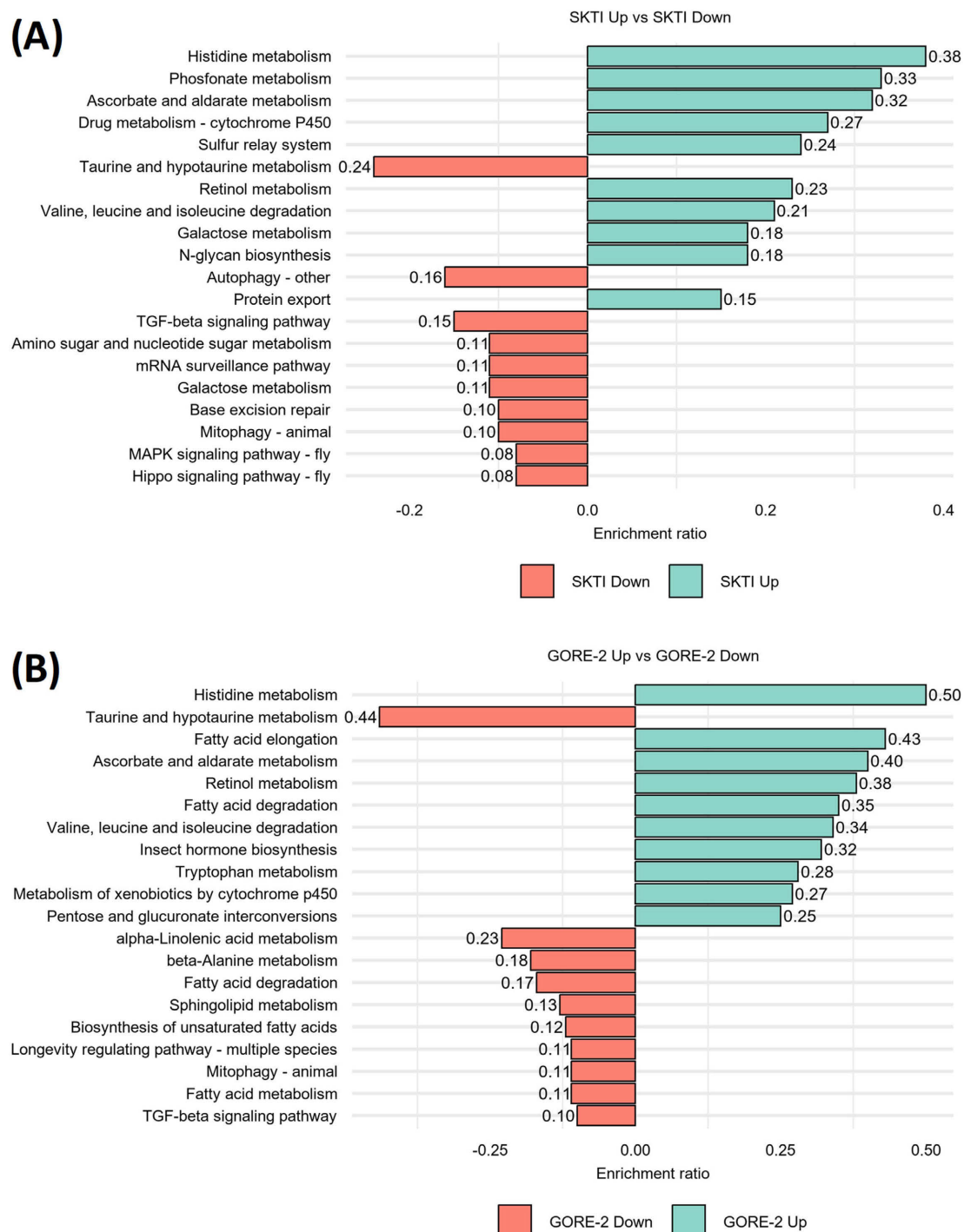


Fig. 5. KEGG pathway enrichment of the top ten most significantly down and up-regulated midgut unigenes of *Anticarsia gemmatilis* following treatment with the natural inhibitor SKTI and the synthetic inhibitor GORE-2. Horizontal bar charts show enrichment ratios (number of mapped DEGs ÷ total annotated unigenes differentially expressed) for each comparison, with values printed at the ends of the bars. Panels are organized as follows: (A) SKTI Down and SKTI Up, with pathways most depleted by both; (B) GORE-2 Down and GORE-2 Up, with pathways most induced by GORE-2. Bars are colored using red for down-regulated enriched pathways, and blue for up-regulated enriched pathways. The statistical thresholds ($FDR < 0.05$, $|\log_2 FC| \geq 1$).

and ascorbate and aldarate metabolism, suggesting an enhanced oxidative and detoxification response. These findings are consistent with elevated oxidative stress and activation of antioxidant defenses in response to the synthetic inhibitor. Also, up-regulated were pathways related to carbohydrate metabolism and lipid metabolism, indicating broader metabolic adjustments beyond proteolysis. Among

down-regulated pathways, GORE-2 strongly affected digestive enzyme activity, including reductions in genes mapped to protein digestion and absorption, reinforcing the inhibitor's suppressive effect on proteolytic capacity.

In contrast, the SKTI vs. Control comparison (Fig. 5A) showed enrichment of up-regulated pathways linked to amino acid biosynthesis, arginine and proline metabolism,

and defense-related responses, but with overall lower enrichment ratios compared to GORE-2. Interestingly, SKTI treatment did not significantly enrich detoxification pathways such as cytochrome P450, highlighting a more limited stress response. Down-regulated pathways under SKTI included those associated with ribosome function and oxidative phosphorylation, suggesting a moderate suppression of energy-related processes.

Altogether, these results indicate that while both inhibitors activate core digestive and immune-related responses, GORE-2 elicits a more extensive metabolic reprogramming, particularly in terms of detoxification, redox balance, and stress signaling, compared to the more localized effects of SKTI. The selective enrichment of detoxification-related pathways under GORE-2 treatment reinforces its potential as a potent modulator of midgut physiology.

4. DISCUSSION

Transcriptome profiling through RNA sequencing (RNA-Seq) is a powerful and widely used approach to explore gene expression regulation and signal transduction pathways in response to biotic and abiotic stimuli (Stark et al., 2019; Wang et al., 2024). In the context of insect physiology, RNA-Seq enables high-resolution analysis of the transcriptional landscape, offering insights into how organisms respond at the molecular level to environmental and dietary challenges. In this study, we employed a transcriptomic strategy to characterize the systemic response of *A. gemmatilis* larvae to dietary protease inhibitors, aiming to identify differentially expressed genes and affected pathways in the midgut, the primary site of digestion and immune surveillance. The rationale for using RNA-Seq stems from the need to uncover not only direct targets of protease inhibition but also secondary signaling cascades and compensatory responses that are not readily detected through proteomics or enzyme activity assays alone. As *A. gemmatilis* lacks a fully sequenced and annotated reference genome, our transcriptome was assembled de novo. However, to improve the accuracy and reliability of functional annotation, we mapped the resulting unigenes against well-characterized Lepidopteran reference proteomes, including *Bombyx mori*, *Danaus plexippus*, and *Heliconius melpomene*, using resources such as UniProt, eggNOG, and KEGG. These comparative annotations allowed us to infer gene function and biological relevance with higher confidence, despite the absence of a species-specific genome.

Synthetic tripeptides with protease inhibitory activity, including GORE-2, were rationally designed based on the sequence of SKTI, a well-characterized Kunitz-type inhibitor from soybean. Previous biochemical data demonstrated that GORE-2 was more effective in reducing both midgut proteolytic activity and larval survival compared to the native SKTI (Barros et al., 2022). Furthermore, studies have shown that SKTI-induced inhibition is transient and partially counteracted by the upregulation of alternate serine protease isoforms, thereby restoring midgut functionality after 24 h (Coura et al., 2022). In contrast, larvae treated

with GORE-2 did not exhibit the same compensatory response, suggesting distinct modes of recognition and signaling. To dissect these differential responses, we performed transcriptomic profiling to compare the molecular cascades triggered by these two PIs when incorporated into the larval diet. While both inhibitors suppressed protease-related pathways, the downstream gene expression programs they induced were clearly distinct.

Treatment with SKTI and GORE-2 resulted in differential expression of several midgut gene families, notably those related to protease activity (KO1312), lipases, and genes involved in tissue repair and immune responses. These results are consistent with known adaptive strategies in insects, where overexpression of proteases or induction of novel isoforms allows partial circumvention of PI activity (Broadway et al., 1997; Zhu-Salzman & Zeng, 2015). While both inhibitors activated this compensatory mechanism, SKTI triggered a more extensive reprogramming of protease gene expression than GORE-2.

Our results suggest that inhibition of intestinal proteases by dietary PIs is compensated by the overexpression of alternative digestive enzymes, including trypsins, chymotrypsins, serine proteases, and aminopeptidases (Coura et al., 2022). Notably, the number of up-regulated genes encoding proteolytic enzymes was higher in response to SKTI treatment. A similar increase in trypsin gene expression in response to PI-induced damage has been reported in *Helicoverpa armigera* (Lomate & Hivrale, 2011; Lomate et al., 2018). Likewise, overexpression of protease-encoding genes has been identified in the midgut transcriptome of *Spodoptera frugiperda* larvae fed on soybean-derived protease inhibitors (Brioschi et al., 2007). However, GORE-2 induced a comparatively lower reprogramming of genes associated with protease activity than SKTI. This observation suggests that transcriptional changes in the caterpillar midgut may not be solely attributed to amino acid deprivation. Furthermore, our findings support the notion that the insect's natural defense system against PIs is only partially activated when challenged with short mimetic peptides like GORE-2, consistent with previous findings (Barros et al., 2022). The reduced expression of protease isoforms in response to GORE-2, relative to SKTI, highlights differences in the efficacy of protease inhibition. This likely reflects the ability of *A. gemmatilis* to detect and respond more strongly to plant-derived inhibitors like SKTI, through a perception and signaling system that governs digestive enzyme expression. This system appears to be only partially activated in response to the synthetic tripeptide GORE-2.

RNASeq has been widely used to identify and elucidate mechanisms by which phytophagous insects respond to PIs effects (Souza et al., 2016; Lin et al., 2017; Lomate et al., 2018) or the use of *Bacillus thuringiensis* toxin (Dhaniala et al., 2019; Pezenti et al., 2021). This tool generates highly reproducible data, enabling precise quantification of expression levels (Schurch et al., 2016). Among the highly expressed transcripts, we identified seven unigenes encoding proteins involved in the repair of the intestinal endothelium.

One unigene encodes chitin deacetylase, an enzyme involved in chitin metabolism that plays an important role in protecting the midgut from mechanical damage, microbial infections, and pathogen invasion (Alvarenga et al., 2016). Unigenes encoding cuticle proteins were also highly expressed; these proteins, in conjunction with chitin, contribute to gut protection by reinforcing the physical barrier associated with the peritrophic matrix (Muthukrishnan et al., 2019). Additionally, treatment with PIs led to increased expression of unigenes encoding mucin glycoproteins (secreted during digestion), which preserve tissue integrity by preventing microbial adhesion and enzymatic degradation of epithelial cells (Fang et al., 2009). Together, these findings suggest that exposure to PIs reprograms gene expression in *A. gemmatalis* midgut cells to enhance protective mechanisms and maintain intestinal homeostasis.

The expression of unigenes encoding peritrophin proteins was up-regulated in response to both GORE-2 and SKTI protease inhibitor treatments. Peritrophins are structural glycoproteins that contribute to the formation of the peritrophic membrane, a key component of the peritrophic matrix (Song et al., 2025). This matrix consists of proteins and glycan components and plays essential roles in protecting the caterpillar midgut. It also helps compartmentalize digestive enzymes released into the gut lumen and contributes to chitin synthesis (Song et al., 2025). Similar findings were reported by Liu et al. (2004), who observed increased expression of peritrophins and chitin-associated proteins in larvae of *Diabrotica undecimpunctata* when exposed to cysteine protease inhibitors.

This response appears to represent a defense mechanism in caterpillars, promoting rapid peritrophic membrane renewal and enhancing protection of the intestinal epithelium. Chitin metabolism and cuticle synthesis are essential not only for structural integrity but also for digestive efficiency and innate immunity in insects. These structures are actively involved in both mechanical and chemical digestion by supporting the function of digestive enzymes (Terra et al., 2009). Studies involving *Helicoverpa armigera* fed diets containing PIs have shown that these inhibitors can accumulate in the peritrophic membrane and intestinal epithelium, where they may interact with protective structures to induce compensatory expression of proteases (Lomate et al., 2018). Furthermore, some studies have highlighted the use of PI-lecithin complexes to enhance cellular damage in the midgut of phytophagous insects (Napoleão et al., 2019). Li et al. (2009) also demonstrated that *Drosophila* exposed to gut injury showed upregulation of genes involved in chitin and cuticle metabolism, suggesting a repair mechanism activated in response to epithelial damage. Consistent with these findings, our results indicate that the immune system of *A. gemmatalis* responds to PI-induced stress by overexpressing genes involved in the synthesis of structural proteins such as chitin, peritrophins, and cuticle proteins to restore midgut integrity.

Other genes strongly induced by protease inhibitors (PIs) encode mucins. Mucins are structural proteins rich in proline, threonine, and serine residues, characterized by

high levels of glycosylation, and are integral components of the insect peritrophic matrix. These proteins serve multiple protective roles in the gut, including shielding intestinal epithelial cells from physical and chemical damage, facilitating food passage through lubrication, preventing dehydration, and protecting against autolysis by digestive enzymes (Toprak et al., 2010). Studies on *Mamestra configurata* larvae at different feeding stages revealed dynamic expression of mucin-associated proteins, suggesting that mucin synthesis and peritrophic matrix architecture are modulated in response to metabolic stress (Toprak et al., 2010). This regulation involves changes in the thickness of the peritrophic matrix and its associated protein composition, influenced by secreted digestive enzymes such as serine proteases and trypsin. Overproduction of these enzymes can trigger autolytic processes and degrade mucins, which are particularly vulnerable due to their serine-rich structure (Toprak et al., 2010; Napoleão et al., 2019).

Several studies have investigated the mechanisms through which protease inhibitors (PIs) interact with the insect digestive system and how insects respond to their anti-nutritional effects and the cellular damage inflicted on the midgut epithelium (Silva-Júnior et al., 2021). These studies have demonstrated that PI exposure activates the insect immune system, leading to increased expression of genes involved in chitin metabolism, peritrophic membrane synthesis, and cuticle remodeling. All of these components contribute to the structural defense of the digestive tract and form part of the peritrophic matrix, which is a key target of PI action (Mohan et al., 2006; Nascimento et al., 2015). The results presented in this study support these findings, indicating that PIs reduce the availability of essential amino acids and disrupt the structural integrity of the peritrophic matrix. In addition to impairing digestion, PI treatments induced oxidative stress in the midgut tissue, as suggested by the gene expression patterns observed. A large number of up-regulated genes were associated with the ascorbate-glutathione pathway, which plays a central role in reactive oxygen species (ROS) detoxification. It is well established that environmental and nutritional stress can lead to ROS accumulation. In this context, the activation of the ascorbate-glutathione cycle appears to be a key biochemical defense mechanism triggered in response to PI-induced oxidative imbalance.

The enrichment levels were higher for pathways related to drug and xenobiotic metabolism by cytochrome P450 enzymes when caterpillars were fed with the protease inhibitor GORE-2. Cytochrome P450 (CYP450), a superfamily of heme-thiolate proteins, is primarily involved in the metabolism of endogenous and exogenous substances, such as pheromones and insecticides. This result aligns with previous findings where GORE-2 exhibited a more pronounced reduction in *A. gemmatalis* survival compared to SKTI. Specifically, Barros et al. (2022) demonstrated that larvae fed with GORE-2 showed a significant decrease in survival rates relative to those treated with SKTI, correlating with increased expression of detoxification-related genes, including members of the CYP450 family.

Additionally, Meriño-Cabrera et al. (2022) reported that arginine-containing dipeptides, such as GORE-2, compromised larval development and survival, further supporting the enhanced efficacy of synthetic peptides over natural inhibitors.

5. CONCLUSION

Dietary exposure to the protease inhibitors SKTI and GORE-2 induced extensive transcriptional reprogramming in the midgut of *A. gemmatilis* larvae after 24 h. Both treatments modulated genes involved in proteolysis and intestinal defense, especially those associated with peritrophic matrix integrity and regeneration. However, SKTI elicited a more pronounced activation of defense-related signaling pathways, suggesting that the native inhibitor is more readily recognized by the insect's midgut defense system. In contrast, GORE-2 treatment led to a more effective inhibition of proteolytic activity and greater reduction in larval survival, despite eliciting a weaker immune response. This may reflect its reduced ability to fully activate plant defense perception pathways, which appear to be triggered not only by amino acid deprivation but also by recognition of plant-derived chemical cues. As a synthetic mimetic tripeptide, GORE-2 likely bypasses key perception checkpoints, resulting in limited activation of compensatory mechanisms.

One notable advantage of synthetic or mimetic inhibitors such as GORE-2 is their ability to induce significant molecular disruptions in the insect midgut. Consistent with previous proteomic findings (Coura et al., 2022), our transcriptomic data revealed strong upregulation of genes associated with xenobiotic metabolism, particularly cytochrome P450s, as well as genes involved in oxidative stress responses. These effects likely contribute to the superior larvicidal activity of GORE-2.

In conclusion, while both SKTI and GORE-2 target digestive physiology and activate defense pathways, their transcriptional footprints are distinct. The broader impact of GORE-2 on detoxification and oxidative stress processes underscores its potential as a promising candidate for the development of peptide-based biopesticides.

ACKNOWLEDGEMENTS. The authors would like to thank to NuBioMol (Center of Analyses of Biomolecules-UFV, Brazil) for the infrastructure and technical assistance. This study was supported by the National Institute of Science and Technology in Plant-Pest Interaction (INCT-IPP), Fundação de Amparo à Pesquisa de Minas Gerais (FAPEMIG), Coordenação de Aperfeiçoamento de Pessoal de Nível Superior (CAPES), and Conselho Nacional de Desenvolvimento Científico e Tecnológico (CNPq).

ETHICS APPROVAL AND CONSENT TO PARTICIPATE. The work did not involve ethical questions and all authors agreed to participate in this research study.

CONSENT FOR PUBLICATION. All authors are in accordance with the publication of the manuscript.

AVAILABILITY OF DATA AND MATERIAL. All authors are in accordance with the publication of the all data and figures.

COMPETING INTERESTS. All authors have no pecuniary or other personal interest.

REFERENCES

- ALTSCHUL S.F., GISH W., MILLER W., MYERS E.W. & LIPMAN D.J. 1990: Basic local alignment search tool. — *J. Mol. Biol.* **215**: 403–410.
- ALVARENGA E.S.L., MANSUR J.F., JUSTI S.A., FIGUEIRA-MANSUR J., DOS SANTOS V.M., LOPEZ S.G., MASUDA H., LARA F.A., MELO A.C.A. & MOREIRA M.F. 2016: Chitin is a component of the *Rhodnius prolixus* midgut. — *Insect Biochem. Mol. Biol.* **69**: 61–70.
- ANDREWS S. 2010: *FastQC – A Quality Control Tool for High Throughput Sequence Data*. URL: <http://www.bioinformatics.babraham.ac.uk/projects/fastqc/>. BabrahamBioinformatics.
- BARROS R.A., MERIÑO-CABRERA Y., CASTRO J.S., SILVA JUNIOR N.R., OLIVEIRA J.V.A., SCHULTZ H., ANDRADE R.J., RAMOS H.J. & OLIVEIRA M.G.A. 2022: Bovine pancreatic trypsin inhibitor and soybean Kunitz trypsin inhibitor: Differential effects on proteases and larval development of the soybean pest *Anticarsia gemmatilis* (Lepidoptera: Noctuidae). — *Pestic. Biochem. Physiol.* **187**: 105188, 12 pp.
- BEL Y., ZACK M., NARVA K., ESCRICHE B. 2019: Specific binding of *Bacillus thuringiensis* cryIIa toxin, and cryIac and CryIFa competition analyses in *Anticarsia gemmatilis* and *Chrysodeixis includens*. — *Sci. Rep.* **9**: 18201, 7 pp.
- BOAVENTURA D., BOLZAN A., PADOVEZ F.E., OKUMA D.M., OMOTO C. & NAUEN R. 2020: Detection of a mutation associated with pyrethroid resistance in the soybean looper, *Chrysodeixis includens*, and its spread in Brazilian populations. — *Pest Manag. Sci.* **76**: 943–950.
- BOLGER A.M., LOHSE M. & USADEL B. 2014: Trimmomatic: A flexible trimmer for Illumina sequence data. — *Bioinformatics* **30**: 2114–2120.
- BRAY N.L., PIMENTEL H., MELSTED P. & PACTER L. 2016: Near-optimal probabilistic RNA-seq quantification. — *Nature Biotechnol.* **34**: 525–527.
- BRIOSCHI D., NADALINI L.D., BENGTSON M.H., SOGAYAR M.C., MOURA D.S. & SILVA-FILHO M.C. 2007: General up regulation of *Spodoptera frugiperda* trypsins and chymotrypsins allows its adaptation to soybean proteinase inhibitor. — *Insect Biochem. Mol. Biol.* **37**: 1283–1290.
- BROADWAY R.M. 1997: Dietary regulation of serine proteinases that are resistant to serine proteinase inhibitors. — *J. Insect Physiol.* **43**: 855–874.
- CAMPOS E.V.R., PROENÇA P.L.F., OLIVEIRA J.L., BAKSHI M., ABHILASH P.C. & FRACETO L.F. 2019: Use of botanical insecticides for sustainable agriculture: Future perspectives. — *Ecol. Indicators* **105**: 483–495.
- CONESA A., GÖTZ S., GARCÍA-GÓMEZ J.M., TEROL J., TALÓN M. & ROBLES M. 2005: Blast2GO: A universal tool for annotation, visualization and analysis in functional genomics research. — *Bioinformatics* **21**: 3674–3676.
- COURA R.R., DA SILVA JUNIOR N.R., MERIÑO-CABRERA Y., DíEZ J.D.R., BARROS R.A., BARBOSA S.L., DE OLIVEIRA J.V.A., DA ROCHA G.C., SERRÃO J.E., DE OLIVEIRA RAMOS H.J. & DE ALMEIDA OLIVEIRA M.G. 2022: Extensive reprogramming of protein isoforms and histopathological alterations in the midgut of *Anticarsia gemmatilis* fed with protease inhibitors. — *Ann. Appl. Biol.* **180**: 383–397.
- DA SILVA FORTUNATO F., DE ALMEIDA OLIVEIRA M.G., BRUMANO M.H.N., SILVA C.H.O., GUEDES R.N.C., MOREIRA M.A. 2007: Lipoxigenase-induced defense of soybean varieties to the attack of the velvetbean caterpillar (*Anticarsia gemmatilis* Hübner). — *J. Pest Sci.* **80**: 241–247.

- DA SILVA-JÚNIOR N.R., VITAL C.E., DE ALMEIDA BARROS R., DE OLIVEIRA E.E., DE OLIVEIRA RAMOS H.J. & DE ALMEIDA OLIVEIRA M.G. 2020: Intestinal proteolytic profile changes during larval development of *Anticarsia gemmatilis* caterpillars. — *Arch. Insect Biochem. Physiol.* **103**: e21631, 14 pp.
- DHANIA N.K., CHAUHAN V.K., CHAITANYA R.K. & DUTTA-GUPTA A. 2019: Midgut de novo transcriptome analysis and gene expression profiling of *Achaea janata* larvae exposed with *Bacillus thuringiensis* (Bt)-based biopesticide formulation. — *Comp. Biochem. Physiol. (D)* **30**: 81–90.
- EDDY S.R. & WHEELER T.J. 2015: *HMMER 3.1.2b*. URL: <http://hmmer.org/>.
- EWELS P., MAGNUSSON M., LUNDIN S. & KÄLLER M. 2016: MultiQC: Summarize analysis results for multiple tools and samples in a single report. — *Bioinformatics* **32**: 3047–3048.
- FANG S., WANG L., GUO W., ZHANG X., PENG D., LUO C., YU Z. & SUN M. 2009: *Bacillus thuringiensis* bel protein enhances the toxicity of Cry1Ac protein to *Helicoverpa armigera* larvae by degrading insect intestinal mucin. — *Appl. Environ. Microbiol.* **75**: 5237–5243.
- FERNANDES F.O., ABREU J.Á. DE, CHRIST L.M. & ROSA A.P.S.A. DA 2018: Insecticides management used in soybean for the control of *Anticarsia gemmatilis* (Hübner, 1818) (Lepidoptera: Eriidae). — *J. Agric. Sci.* **10**: 223–230.
- FINN R.D., BATEMAN A., CLEMENTS J., COGGILL P., EBERHARDT R.Y., EDDY S.R., HEGER A., HETHERINGTON K., HOLM L., MISTRY J., SONNHAMMER E.L.L., TATE J. & PUNTA M. 2014: Pfam: The protein families database. — *Nucl. Acids Res.* **42**: D222–D230.
- FU L., NIU B., ZHU Z., WU S. & LI W. 2012: CD-HIT: Accelerated for clustering the next-generation sequencing data. — *Bioinformatics* **28**: 3150–3152.
- GRABHERR M.G., HAAS B.J., YASSOUR M., LEVIN J.Z., THOMPSON D.A., AMIT I., ADICONIS X., FAN L., RAYCHOWDHURY R., ZENG Q., CHEN Z., MAUCELI E., HACHOEN N., GNIRKE A., RHIND N., DI PALMA F., BIRREN B.W., NUSBAUM C., LINDBLAD-TOH K. ... REGEV A. 2011: Full-length transcriptome assembly from RNA-Seq data without a reference genome. — *Nature Biotechnol.* **29**: 644–652.
- HAAS B.J., PAPANICOLAOU A., YASSOUR M., GRABHERR M., BLOOD P.D., BOWDEN J., COUGER M.B., ECCLES D., LI B., LIEBER M., MACMANES M.D., OTT M., ORVIS J., POCHE T. N., STROZZI F., WEEKS N., WESTERMAN R., WILLIAM T., DEWEY C.N. ... REGEV A. 2013: De novo transcript sequence reconstruction from RNA-seq using the Trinity platform for reference generation and analysis. — *Nature Protocols* **8**: 1494–1512.
- HUERTA-CEPAS J., SZKLARCZYK D., FORSLUND K., COOK H., HELLER D., WALTER M.C., RATTEI T., MENDE D.R., SUNAGAWA S., KUHN M. ET AL. 2016: eggNOG 4.5: a hierarchical orthology framework with improved functional annotations for eukaryotic, prokaryotic and viral sequences. — *Nucl. Acids Res.* **44**: D286–D293.
- HUERTA-CEPAS J., FORSLUND K., COELHO L.P., SZKLARCZYK D., JENSEN L.J., VON MERING C. & BORK P. 2017: Fast genome-wide functional annotation through orthology assignment by eggNOG-mapper. — *Mol. Biol. Evol.* **34**: 2115–2122.
- KRUEGER F. 2021: *TrimGalore*. URL: <https://Github.Com/FelixKrueger/TrimGalore#readme>.
- KUWAR S.S., PAUCHET Y., VOGEL H. & HECKEL D.G. 2015: Adaptive regulation of digestive serine proteases in the larval midgut of *Helicoverpa armigera* in response to a plant protease inhibitor. — *Insect Biochem. Mol. Biol.* **59**: 18–29.
- LANGMEAD B. & SALZBERG S.L. 2012: Fast gapped-read alignment with Bowtie 2. — *Nature Meth.* **9**: 357–359.
- LI H.M., SUN L., MITTAPALLI O., MUIR W.M., XIE J., WU J., SCHEMERHORN B.J., SUN W., PITTENDRIGH B.R. & MURDOCK L.L. 2009: Transcriptional signatures in response to wheat germ agglutinin and starvation in *Drosophila melanogaster* larval midgut. — *Insect Mol. Biol.* **18**: 21–23.
- LIMA B.S.A., ROCHA F.A.D., PLATA-RUEDA A., ZANUNCIO J.C., COSSOLIN J.F.S., MARTÍNEZ L.C. & SERRÃO J.E. 2024: Abamectin induces mortality, inhibits food consumption, and causes histological changes in the midgut of the velvetbean caterpillar *Anticarsia gemmatilis* (Lepidoptera: Noctuidae). — *J. Pest Sci.* **97**: 213–227.
- LIN H., LIN X., ZHU J., YU X.Q., XIA X., YAO F., YANG G. & YOU M. 2017: Characterization and expression profiling of serine protease inhibitors in the diamondback moth, *Plutella xylostella* (Lepidoptera: Plutellidae). — *BMC Genomics* **18**: 162, 13 pp.
- LIU Y., SALZMAN R.A., PANKIW T. & ZHU-SALZMAN K. 2004: Transcriptional regulation in southern corn rootworm larvae challenged by soyacystatin N. — *Insect Biochem. Mol. Biol.* **34**: 1069–1077.
- LOMATE P.R. & HIVRALE V.K. 2011: Differential responses of midgut soluble aminopeptidases of *Helicoverpa armigera* to feeding on various host and non-host plant diets. — *Arthr.-Plant Interact.* **5**: 359–368.
- LOMATE P.R., DEWANGAN V., MAHAJAN N.S., KUMAR Y., KULKARNI A., WANG L., SAXENA S., GUPTA V.S. & GIRI A.P. 2018: Integrated transcriptomic and proteomic analyses suggest the participation of endogenous protease inhibitors in the regulation of protease gene expression in *Helicoverpa armigera*. — *Mol. Cell. Proteomics* **17**: 1324–1336.
- LOVE M.I., HUBER W. & ANDERS S. 2014: Moderated estimation of fold change and dispersion for RNA-seq data with DESeq2. — *Genome Biol.* **15**: 550, 21 pp.
- MAHANTA D.K., KOMAL J., SAMAL I., BHOI T.K., KUMAR P.V.D., MOHAPATRA S., ATHULYA R., MAJHI P.K. & MASTINU A. 2025: Plant defense responses to insect herbivores through molecular signaling, secondary metabolites, and associated epigenetic regulation. — *Plant-Environ. Interact.* **6**: e70035, 18 pp.
- MENDONÇA E.G., DE ALMEIDA BARROS R., CORDEIRO G., DA SILVA C.R., CAMPOS W.G., DE OLIVEIRA J.A. & DE ALMEIDA OLIVEIRA M.G. 2020: Larval development and proteolytic activity of *Anticarsia gemmatilis* Hübner (Lepidoptera: Noctuidae) exposed to different soybean protease inhibitors. — *Arch. Insect Biochem. Physiol.* **103**: e21637, 9 pp.
- MERIÑO-CABRERA Y., ZANUNCIO J.C., SILVA R.S., SOLIS-VARGAS M., CORDEIRO G., RIBEIRO F.R., CAMPOS W.G., PÍCANÇO M.C. & OLIVEIRA M.G.A. 2018: Biochemical response between insects and plants: an investigation of enzyme activity in the digestive system of *Leucoptera coffeella* (Lepidoptera: Lyonetiidae) and leaves of *Coffea arabica* (Rubiaceae) after herbivory. — *Ann. Appl. Biol.* **172**: 236–243.
- MERIÑO-CABRERA Y., CASTRO J.S., BARROS R.A., SILVA JUNIOR N.R., RAMOS H.J. & OLIVEIRA M.G.A. 2022: Arginine-containing dipeptides decrease affinity of gut trypsins and compromise soybean pest development. — *Pestic. Biochem. Physiol.* **187**: 105107, 10 pp.
- MOHAN S., MA P.W.K., PECHAN T., BASSFORD E.R., WILLIAMS W.P. & LUTHE D.S. 2006: Degradation of the *S. frugiperda* peritrophic matrix by an inducible maize cysteine protease. — *J. Insect Physiol.* **52**: 21–28.
- MUTHUKRISHNAN S., MERZENDORFER H., ARAKANE Y. & YANG Q. 2019: Chitin organizing and modifying enzymes and proteins involved in remodeling of the insect cuticle. In Yang Q. & Fukamizo T. (eds): *Targeting Chitin-containing Organisms*.

- Advances in Experimental Medicine and Biology*, Vol. 1142. Springer, Singapore, pp. 83–114.
- NAPOLÉÃO T.H., ALBUQUERQUE L.P., SANTOS N.D., NOVA I.C., LIMA T.A., PAIVA P.M. & PONTUAL E.V. 2019: Insect midgut structures and molecules as targets of plant-derived protease inhibitors and lectins. — *Pest Manag. Sci.* **75**: 1212–1222.
- NASCIMENTO A.R.B., DO FRESIA P., CÔNSOLI F.L. & OMOTO C. 2015: Comparative transcriptome analysis of lufenuron-resistant and susceptible strains of *Spodoptera frugiperda* (Lepidoptera: Noctuidae). — *BMC Genomics* **16**: 985: 12 pp.
- PEZENTI L.F., SOSA-GÓMEZ D.R., DE SOUZA R.F., VILAS-BOAS L.A., GONÇALVES K.B., DA SILVA C.R.M., VILAS-BÔAS G.T., BARANOSKI A., MANTOVANI M.S. & DA ROSA R. 2021: Transcriptional profiling analysis of susceptible and resistant strains of *Anticarsia gemmatalis* and their response to *Bacillus thuringiensis*. — *Genomics* **113**: 2264–2275.
- PLATA-RUEDA A., DE MENEZES C.H.M., CUNHA W.D., ALVARENGA T.M., BARBOSA B.F., ZANUNCIO J.C. & SERRÃO J.E. 2020: Side-effects caused by chlorpyrifos in the velvetbean caterpillar *Anticarsia gemmatalis* (Lepidoptera: Noctuidae). — *Chemosphere* **259**: 127530, 7 pp.
- PONNUVEL P., NARAYANANKUTTY K., JALALUDEEN A. & ANITHA P. 2015: Effect of phytase supplementation in low energy-protein diet on the production performance of layer chicken. — *Int. J. Vet. Sci. Biotechnol.* **3**: 25–27.
- QU J., JIN Y., WU J. & MENG Y. 2022: Challenges and prospects of bioinsecticides in sustainable pest management. — *Front. Agric. Sci. Engin.* **9**: 108–120.
- ROY D., MOUGHAN P.J., YE A., HODGKINSON S.M., STROEBINGER N., LI S., DAVE A.C., MONTOYA C.A. & SINGH H. 2022: Structural changes in milk from different species during gastric digestion in piglets. — *J. Dairy Sci.* **105**: 3810–3831.
- SCHURCH N.J., SCHOFIELD P., GIERLIŃSKI M., COLE C., SHERSTNEV A., SINGH V., WROBEL N., GHARBI K., SIMPSON G.G., OWEN-HUGHES T., BLAXTER M. & BARTON G.J. 2016: How many biological replicates are needed in an RNA-seq experiment and which differential expression tool should you use? — *RNA* **22**: 839–851.
- SHAKEEL M. & ZAFAR J. 2020: Molecular identification, characterization, and expression analysis of a novel trypsin inhibitor-like cysteine-rich peptide from the cotton bollworm, *Helicoverpa armigera* (Hübner) (Lepidoptera: Noctuidae). — *Egypt. J. Biol. Pest Contr.* **30**: 10, 7 pp.
- SILVA-JÚNIOR N.R., CABRERA Y.M., BARBOSA S.L., BARROS R. DE A., BARROS E., VITAL C.E., RAMOS H.J.O. & OLIVEIRA M.G.A. 2021: Intestinal proteases profiling from *Anticarsia gemmatalis* and their binding to inhibitors. — *Arch. Insect Biochem. Physiol.* **107**: e21792, 28 pp.
- SONG L. & FLOREA L. 2015: Rcorrector: Efficient and accurate error correction for Illumina RNA-seq reads. — *GigaScience* **4**: 48, 8 pp.
- SONG X., AN J., ZHOU Z., LI Z., WANG X., WANG Y. & WANG S. 2025: Gut bacterial components modulate Per1 expression and peritrophic matrix structure in *Anopheles stephensi*. — *PLoS Pathog.* **21**: e1010843, 26 pp.
- SOUZA T.P., DIAS R.O., CASTELHANO E.C., BRANDÃO M.M., MOURA D.S. & SILVA-FILHO M.C. 2016: Comparative analysis of expression profiling of the trypsin and chymotrypsin genes from Lepidoptera species with different levels of sensitivity to soybean peptidase inhibitors. — *Comp. Biochem. Physiol. (B)* **196–197**: 67–73.
- STARK R., GRZELAK M. & HADFIELD J. 2019: RNA sequencing: the teenage years. — *Nat. Rev. Genet.* **20**: 631–656.
- TERRA W.T. & FERREIRA C. 2012: Biochemistry and molecular biology of digestion. In Gilbert L.I. (ed.): *Insect Molecular Biology and Biochemistry*. Elsevier Academic Press, Amsterdam, pp. 365–418.
- TERRA X., MONTAGUT G., BUSTOS M., LLOPÍZ N., ARDEVOL A., BLADÉ C., FERNÁNDEZ-LARREA J., PUJADAS G., SALVADÓ J., AROLA L. & BLAY M. 2009: Grape-seed procyanidins prevent low-grade inflammation by modulating cytokine expression in rats fed a high-fat diet. — *J. Nutr. Biochem.* **20**: 210–218.
- TOPRAK U., BALDWIN D., ERLANDSON M., GILLOTT C. & HEGEDUS D.D. 2010: Insect intestinal mucins and serine proteases associated with the peritrophic matrix from feeding, starved and moulting *Mamestra configurata* larvae. — *Insect Mol. Biol.* **19**: 163–175.
- TOPRAK U., ERLANDSON M., BALDWIN D., KARCZ S., WAN L., COUTU C., GILLOTT C. & HEGEDUS D.D. 2015: Identification of the *Mamestra configurata* (Lepidoptera: Noctuidae) peritrophic matrix proteins and enzymes involved in peritrophic matrix chitin metabolism. — *Insect Sci.* **23**: 656–674.
- VAN BEL M., PROOST S., VAN NESTE C., DEFORCE D., VAN DE PEER Y. & VANDEPOELE K. 2013: TRAPID: An efficient online tool for the functional and comparative analysis of de novo RNA-Seq transcriptomes. — *Genome Biology* **14**: R134, 10 pp.
- VISOTTO L.E., OLIVEIRA M.G., RIBON A.O., MARES-GUIA T.R. & GUEDES R.N. 2009: Characterization and identification of proteolytic bacteria from the gut of the velvetbean caterpillar (Lepidoptera: Noctuidae). — *Environ. Entomol.* **38**: 1078–1085.
- WANG J., GERMINARA G.S., FENG Z., LUO S., YANG S., XU S., LI C. & CAO Y. 2022: Comparative effects of heat and cold stress on physiological enzymes in *Sitophilus oryzae* and *Lasioderma serricorne*. — *J. Stored Prod. Res.* **96**: 101948, 8 pp.
- WANG H., CHEN Z., LUO R., LEI C., ZHANG M., GAO A., PU J. & ZHANG H. 2024: Caffeic acid O-methyltransferase gene family in mango (*Mangifera indica* L.) with transcriptional analysis under biotic and abiotic stresses and the role of MiCOMT1 in salt tolerance. — *Int. J. Mol. Sci.* **25**: 2639, 18 pp.
- XIE C., MAO X., HUANG J., DING Y., WU J., DONG S., KONG L., GAO G., LI C.Y. & WEI L. 2011: KOBAS 2.0: A web server for annotation and identification of enriched pathways and diseases. — *Nucl. Acids Res. (Suppl. 2)* **39**: W316–W322.
- ZHANG Y.-J., FENG M.-G., FAN Y.-H., LUO Z.-B., YANG X.-Y., WU D. & PEI Y. 2008: A cuticle-degrading protease (CDEP-1) of *Beauveria bassiana* enhances virulence. — *Biocontr. Sci. Technol.* **18**: 551–563.
- ZHAO A., LI Y., LENG C., WANG P. & LI Y. 2019: Inhibitory effect of protease inhibitors on larval midgut protease activities and the performance of *Plutella xylostella* (Lepidoptera: Plutellidae). — *Front. Physiol.* **9**: 1963, 9 pp.
- ZHU-SALZMAN K. & ZENG R. 2015: Insect response to plant defensive protease inhibitors. — *Annu. Rev. Entomol.* **60**: 233–252.

Received February 3, 2025; revised and accepted June 2, 2025
Published online July 2, 2025

Table S1. *A. gemmatalis* reference assembly statistics.

Score	
Total trinity 'genes'	20,192
Total trinity transcripts	51,825
Percent GC	40.41
Statistics based on all transcripts	
Contig N50	3,246
Median contig length	1,617
Average contig	2,243.60
Total assembled bases	116,274,451
Statistics based on longest isoform per 'gene'	
Contig N50	2,891
Median contig length	1,204
Average contig	1906.23
Total assembled bases	38,490,674

Table S2. Top differentially expressed genes (DEGs) in *Anticarsia gemmatilis* midguts from the SKTI vs. Control comparison, ranked by statistical significance.

ID	Uniprot	BaseMean	log2Fold	lfcSE	stat	pvalue	padj	Description
TRINITY_DN527_c0_g1_i3	A0A2H1VM91	6759,572	29,35388432	3,906746	7,51364	5,75E-14	4,58E-11	Alpha-amylase OS=Spodoptera frugiperda OX=7108 GN=SFRICE_013669 PE=3 SV=1
TRINITY_DN9416_c0_g1_i10	A0A2A4JES0	3872,775	28,67985758	3,90675	7,341105	2,12E-13	1,28E-10	Lipase domain-containing protein OS=Heliothis virescens OX=7102 GN=B5V51_2827 PE=3 SV=1
TRINITY_DN1005_c0_g1_i2	A0A2W1BVT3	3687,171	28,4369094	3,906751	7,278915	3,37E-13	1,91E-10	Ascorbate ferrioreductase (transmembrane) OS=Helicoverpa armigera OX=29058 GN=HaOG202999 PE=4 SV=1
TRINITY_DN690_c0_g1_i2	H9J4W0	802,8151	26,0861065	3,90679	6,67712	2,44E-11	8,15E-09	SH3 domain-containing protein OS=Bombyx mori OX=7091 PE=3 SV=1
TRINITY_DN672_c0_g1_i9	A0A2A4IU12	649,6746	25,90005588	3,9068	6,629481	3,37E-11	1,05E-08	Uncharacterized protein OS=Heliothis virescens OX=7102 GN=B5V51_14059 PE=3 SV=1
TRINITY_DN428_c0_g1_i7	A0A2W1BMB0	1671,088	25,68216635	3,906803	6,573703	4,91E-11	1,47E-08	Uncharacterized protein OS=Helicoverpa armigera OX=29058 GN=HaOG210540 PE=3 SV=1
TRINITY_DN232_c0_g1_i5	A0A2A4K771	483,3908	25,48048938	3,90682	6,522053	6,94E-11	1,97E-08	Cytochrome b5 heme-binding domain-containing protein OS=Heliothis virescens OX=7102 GN=B5V51_11135 PE=4 SV=1
TRINITY_DN2141_c0_g1_i4	A0A2W1C0Z7	394,3216	25,16863504	3,90684	6,442198	1,18E-10	2,99E-08	Ascorbate ferrioreductase (transmembrane) OS=Helicoverpa armigera OX=29058 GN=HaOG202997 PE=4 SV=1
TRINITY_DN3468_c0_g1_i2	A0A2H1W6V8	298,0542	24,79833902	3,367272	7,364518	1,78E-13	1,12E-10	SFRICE_028725 OS=Spodoptera frugiperda OX=7108 GN=SFRICE_028725 PE=4 SV=1
TRINITY_DN920_c0_g1_i8	A0A7E5VSU9	626,8236	24,49637362	3,783865	6,473902	9,55E-11	2,54E-08	solute carrier family 12 member 8 OS=Trichoplusia ni OX=7111 GN=LOC113496414 PE=4 SV=1
TRINITY_DN66_c0_g1_i3	A0A6J2KAS1	167,1658	24,13050681	3,906953	6,176299	6,56E-10	1,37E-07	AMP deaminase OS=Bombyx mandarina OX=7092 GN=LOC114248401 PE=3 SV=1
TRINITY_DN2479_c0_g1_i3	A0A2A4J4T7	399,3458	23,95076072	3,762763	6,365207	1,95E-10	4,68E-08	Peptidase_M14 domain-containing protein OS=Heliothis virescens OX=7102 GN=B5V51_6740 PE=3 SV=1
TRINITY_DN1266_c0_g1_i9	A0A835G6L2	201,1602	23,68524947	3,907019	6,062231	1,34E-09	2,62E-07	UTP--glucose-1-phosphate uridylyltransferase OS=Spodoptera exigua OX=7107 GN=HW555_012720 PE=3 SV=1
TRINITY_DN3150_c0_g1_i4	A0A835GKM6	370,8963	23,6395473	3,907023	6,050527	1,44E-09	2,78E-07	RNA-binding protein 8A OS=Spodoptera exigua OX=7107 GN=HW555_004237 PE=3 SV=1
TRINITY_DN2408_c0_g1_i2	A0A6J1WRC3	133,1594	23,58414331	3,907049	6,036306	1,58E-09	3,01E-07	phosphatase and actin regulator 4 isoform X4 OS=Galleria mellonella OX=7137 GN=LOC113517526 PE=4 SV=1
TRINITY_DN4759_c0_g1_i1	A0A2A4JBT9	103,4092	23,50289198	2,948861	7,970158	1,58E-15	2,42E-12	Uncharacterized protein OS=Heliothis virescens OX=7102 GN=B5V51_3978 PE=4 SV=1
TRINITY_DN2308_c0_g1_i13	A0A7E5WIC0	118,0125	23,45316519	3,907081	6,002733	1,94E-09	3,64E-07	neurobeachin isoform X3 OS=Trichoplusia ni OX=7111 GN=LOC113502961 PE=4 SV=1
TRINITY_DN9900_c0_g1_i9	A0A7E5VDB7	198,6935	23,41960656	3,907079	5,994147	2,05E-09	3,82E-07	uncharacterized protein LOC113492785 OS=Trichoplusia ni OX=7111 GN=LOC113492785 PE=4 SV=1
TRINITY_DN3079_c0_g2_i11	A0A2H1V995	125,5971	23,39237627	3,907081	5,987174	2,14E-09	3,93E-07	SFRICE_010949 OS=Spodoptera frugiperda OX=7108 GN=SFRICE_010949 PE=4 SV=1
TRINITY_DN2406_c0_g1_i9	A0A2W1BZL3	109,4278	23,38911592	3,118602	7,499872	6,39E-14	4,77E-11	TMF_TATA_bd domain-containing protein OS=Helicoverpa armigera OX=29058 GN=HaOG217267 PE=4 SV=1
TRINITY_DN61_c0_g2_i12	A0A7E5WM93	4934,117	-29,94986999	3,906757	-7,66617	1,77E-14	1,82E-11	chymotrypsin-2-like OS=Trichoplusia ni OX=7111 GN=LOC113503911 PE=4 SV=1
TRINITY_DN1380_c0_g1_i2	A0A2A4K3Q9	1533,397	-28,2386155	3,906768	-7,22813	4,90E-13	2,63E-10	MFS domain-containing protein OS=Heliothis virescens OX=7102 GN=B5V51_3335 PE=4 SV=1
TRINITY_DN607_c0_g1_i4	A0A7E5X4B2	1797,024	-28,06261198	3,906768	-7,18308	6,82E-13	3,56E-10	prion-like-(Q/N-rich) domain-bearing protein 25 OS=Trichoplusia ni OX=7111 GN=LOC113509016 PE=4 SV=1
TRINITY_DN266_c0_g1_i1	A0A437B5H9	771,9339	-27,17132593	3,390727	-8,01342	1,12E-15	1,93E-12	Serine/threonine-protein phosphatase OS=Chilo suppressalis OX=168631 GN=evm_009908 PE=3 SV=1
TRINITY_DN1107_c0_g1_i3	A0A7E5VW56	408,3063	-26,13210294	3,528235	-7,40657	1,30E-13	8,37E-11	Tubulin-folding cofactor C OS=Trichoplusia ni OX=7111 GN=LOC113497281 PE=3 SV=1
TRINITY_DN2282_c0_g2_i1	A0A7E5VW61	315,7642	-25,90022625	3,342698	-7,7483	9,31E-15	1,09E-11	ribonuclease Oy OS=Trichoplusia ni OX=7111 GN=LOC113497283 PE=3 SV=1
TRINITY_DN23_c0_g1_i9	A0A7E5VVT5	306,1712	-25,85564042	3,365153	-7,68335	1,55E-14	1,70E-11	TBC1 domain family member 15 isoform X6 OS=Trichoplusia ni OX=7111 GN=LOC113497212 PE=4 SV=1
TRINITY_DN2125_c0_g2_i3	A0A7E5W948	1031,82	-25,83572019	3,906849	-6,61293	3,77E-11	1,14E-08	uncharacterized protein LOC113500211 OS=Trichoplusia ni OX=7111 GN=LOC113500211 PE=4 SV=1
TRINITY_DN4029_c0_g1_i2	A0A2W1BY38	492,574	-25,83020202	2,775232	-9,3074	1,31E-20	1,25E-16	Protein quiver OS=Helicoverpa armigera OX=29058 GN=HaOG202542 PE=3 SV=1
TRINITY_DN339_c0_g1_i3	A0A7E5VP18	324,6755	-25,73843667	3,369008	-7,63977	2,18E-14	2,13E-11	2-aminoethanethiol dioxygenase OS=Trichoplusia ni OX=7111 GN=LOC113495500 PE=4 SV=1
TRINITY_DN674_c0_g1_i2	A0A2A4JDG0	371,8158	-25,49892232	3,906872	-6,52668	6,72E-11	1,93E-08	CHK domain-containing protein OS=Heliothis virescens OX=7102 GN=B5V51_3924 PE=4 SV=1
TRINITY_DN1588_c0_g1_i6	A0A2A4JVJ5	234,7364	-25,29098069	3,906895	-6,47342	9,58E-11	2,54E-08	Uncharacterized protein OS=Heliothis virescens OX=7102 GN=B5V51_11725 PE=3 SV=1
TRINITY_DN782_c0_g2_i3	A0A7E5WTK0	263,8515	-25,28204351	3,126981	-8,08513	6,21E-16	1,16E-12	transcription factor MafK isoform X2 OS=Trichoplusia ni OX=7111 GN=LOC113505201 PE=4 SV=1
TRINITY_DN1147_c0_g1_i9	A0A2A4JR56	204,1739	-25,20420861	3,355514	-7,51128	5,86E-14	4,58E-11	1,4-beta-N-acetylmuramidase OS=Heliothis virescens OX=7102 GN=B5V51_13559 PE=3 SV=1
TRINITY_DN983_c0_g1_i3	A0A7E5W7E3	212,4425	-25,19398443	3,906883	-6,44861	1,13E-10	2,91E-08	uncharacterized protein LOC113500097 isoform X2 OS=Trichoplusia ni OX=7111 GN=LOC113500097 PE=4 SV=1
TRINITY_DN6318_c0_g2_i14	A0A7E5VPI1	207,7038	-25,15341243	3,906908	-6,43819	1,21E-10	3,03E-08	GlcNAc kinase OS=Trichoplusia ni OX=7111 GN=LOC113495493 PE=3 SV=1
TRINITY_DN2293_c0_g1_i2	A0A7E5WA32	181,1954	-25,04335306	3,906918	-6,41	1,46E-10	3,58E-08	PH and SEC7 domain-containing protein 1 OS=Trichoplusia ni OX=7111 GN=LOC113500805 PE=4 SV=1
TRINITY_DN2433_c0_g1_i6	A0A7E5W811	225,1206	-24,85162588	3,906948	-6,36088	2,01E-10	4,75E-08	myosin light chain kinase, smooth muscle-like isoform X2 OS=Trichoplusia ni OX=7111 GN=LOC113500367 PE=4 SV=1
TRINITY_DN1596_c0_g1_i11	A0A7E5VFN7	133,895	-24,74247714	3,906964	-6,33292	2,41E-10	5,52E-08	uncharacterized protein LOC113493354 isoform X4 OS=Trichoplusia ni OX=7111 GN=LOC113493354 PE=4 SV=1
TRINITY_DN7697_c0_g1_i6	A0A835L7P9	127,5466	-24,66499019	3,906973	-6,31307	2,74E-10	6,24E-08	Uncharacterized protein OS=Spodoptera exigua OX=7107 GN=HW555_001826 PE=4 SV=1

Table S3. Top differentially expressed genes (DEGs) in *Anticarsia gemmatilis* midguts from the SKTI vs. Control comparison, ranked by statistical significance.

ID	ID uniprot	BaseMean	log2Fold	lfcSE	stat	pvalue	padj	Description
TRINITY_DN428_c0_g1_i7	A0A2W1BMB0	1671,088	26,91733	3,906772	6,889915	5,58E-12	2,45E-09	Uncharacterized protein OS=Helicoverpa armigera OX=29058 GN=HaOG210540 PE=3 SV=1
TRINITY_DN25_c0_g1_i8	A0A2W1BUB3	537,2302	25,75638	3,906815	6,59268	4,32E-11	1,33E-08	Copper transport protein OS=Helicoverpa armigera OX=29058 GN=HaOG204103 PE=3 SV=1
TRINITY_DN920_c0_g1_i8	A0A7E5VSU9	626,8236	25,55892	3,783795	6,754837	1,43E-11	5,45E-09	solute carrier family 12 member 8 OS=Trichoplusia ni OX=7111 GN=LOC113496414 PE=4 SV=1
TRINITY_DN1005_c0_g1_i2	A0A2W1BVT3	3687,171	25,32947	3,906835	6,483372	8,97E-11	2,41E-08	Ascorbate ferrioreductase (transmembrane) OS=Helicoverpa armigera OX=29058 GN=HaOG202999 PE=4 SV=1
TRINITY_DN3121_c0_g1_i10	A0A2A4K7G1	312,8795	24,89329	3,906881	6,371653	1,87E-10	4,60E-08	Vacuolar fusion protein MON1 homolog OS=Heliothis virescens OX=7102 GN=B5V51_10784 PE=3 SV=1
TRINITY_DN3150_c0_g1_i4	A0A835GKM6	370,8963	24,88605	3,906879	6,369805	1,89E-10	4,62E-08	RNA-binding protein 8A OS=Spodoptera exigua OX=7107 GN=HW555_004237 PE=3 SV=1
TRINITY_DN2479_c0_g1_i3	A0A2A4J4T7	399,3458	24,87493	3,762672	6,610975	3,82E-11	1,19E-08	Peptidase_M14 domain-containing protein OS=Heliothis virescens OX=7102 GN=B5V51_6740 PE=3 SV=1
TRINITY_DN527_c0_g1_i3	A0A2H1VM91	6759,572	24,4114	3,906909	6,248264	4,15E-10	9,65E-08	Alpha-amylase OS=Spodoptera frugiperda OX=7108 GN=SFRICE_013669 PE=3 SV=1
TRINITY_DN1272_c0_g1_i2	A0A7E5WDP5	188,2763	24,39162	3,906948	6,243139	4,29E-10	9,85E-08	atlastin-like isoform X1 OS=Trichoplusia ni OX=7111 GN=LOC113501762 PE=3 SV=1
TRINITY_DN757_c0_g1_i9	A0A7E5X4S8	181,6832	24,3795	3,90695	6,240035	4,37E-10	9,99E-08	GlcNAc-PI synthesis protein OS=Trichoplusia ni OX=7111 GN=LOC113508556 PE=4 SV=1
TRINITY_DN7965_c0_g1_i9	A0A2H1X3G7	179,1555	24,26547	3,906965	6,210823	5,27E-10	1,20E-07	SFRICE_035493 OS=Spodoptera frugiperda OX=7108 GN=SFRICE_035493 PE=3 SV=1
TRINITY_DN920_c0_g1_i5	A0A7E5VSU9	216,8927	24,2609	3,486331	6,958862	3,43E-12	1,59E-09	solute carrier family 12 member 8 OS=Trichoplusia ni OX=7111 GN=LOC113496414 PE=4 SV=1
TRINITY_DN2482_c0_g1_i15	W5VY22	213,7132	24,2177	3,906968	6,198593	5,70E-10	1,26E-07	Cytochrome P450 CYP6AN15v1 OS=Lymantia dispar OX=13123 GN=CYP6AN15v1 PE=2 SV=1
TRINITY_DN690_c0_g1_i2	H9J4W0	802,8151	24,17532	3,906955	6,187765	6,10E-10	1,34E-07	SH3 domain-containing protein OS=Bombyx mori OX=7091 PE=3 SV=1
TRINITY_DN3633_c2_g1_i5	A0A7E5VYM3	159,173	24,08298	3,107743	7,749346	9,24E-15	8,59E-12	lysosomal alpha-glucosidase-like OS=Trichoplusia ni OX=7111 GN=LOC113497839 PE=3 SV=1
TRINITY_DN4530_c0_g2_i3	A0A7E5VTU1	157,0495	24,04893	3,138717	7,662023	1,83E-14	1,59E-11	ADP-ribosylation factor-like protein 4C OS=Trichoplusia ni OX=7111 GN=LOC113496513 PE=3 SV=1
TRINITY_DN600_c0_g1_i18	A0A3Q0JKU4	149,6004	24,01987	3,907009	6,147892	7,85E-10	1,64E-07	RNA-directed DNA polymerase OS=Diaphorina citri OX=121845 GN=LOC103524063 PE=4 SV=1
TRINITY_DN920_c0_g1_i4	A0A7E5VSU9	182,3688	24,00621	3,55648	6,749993	1,48E-11	5,53E-09	solute carrier family 12 member 8 OS=Trichoplusia ni OX=7111 GN=LOC113496414 PE=4 SV=1
TRINITY_DN1544_c0_g1_i2	A0A7E5VTG2	206,2349	23,87849	3,907024	6,111682	9,86E-10	2,00E-07	uncharacterized protein LOC113496429 OS=Trichoplusia ni OX=7111 GN=LOC113496429 PE=4 SV=1
TRINITY_DN83_c0_g1_i5	A0A2H1V9Y5	170,5134	23,76975	3,907048	6,083814	1,17E-09	2,33E-07	SFRICE_003033 OS=Spodoptera frugiperda OX=7108 GN=SFRICE_003033 PE=3 SV=1
TRINITY_DN61_c0_g2_i12	A0A7E5WMM93	4934,117	-29,7543	3,906757	-7,61611	2,61E-14	2,12E-11	chymotrypsin-2-like OS=Trichoplusia ni OX=7111 GN=LOC113503911 PE=4 SV=1
TRINITY_DN9184_c0_g1_i9	A0A2A4JX80	5569,469	-29,0916	3,906758	-7,44648	9,59E-14	6,84E-11	Peptidase S1 domain-containing protein (Fragment) OS=Heliothis virescens OX=7102 GN=B5V51_10501 PE=4 SV=1
TRINITY_DN97_c0_g1_i2	A0A2W1BHW2	2592,96	-28,8575	3,906762	-7,38656	1,51E-13	1,01E-10	Uncharacterized protein OS=Helicoverpa armigera OX=29058 GN=HaOG208738 PE=4 SV=1
TRINITY_DN553_c0_g1_i3	A0A2H1V3K8	5019,246	-28,6752	3,906763	-7,33988	2,14E-13	1,36E-10	SFRICE_022831 OS=Spodoptera frugiperda OX=7108 GN=SFRICE_022831 PE=4 SV=1
TRINITY_DN4227_c0_g1_i1	D0ENK2	2960,852	-27,9712	3,835627	-7,29248	3,04E-13	1,87E-10	Ornithine decarboxylase OS=Spodoptera litura OX=69820 PE=2 SV=1
TRINITY_DN3438_c0_g1_i7	A0A835G5G4	458,128	-26,1872	3,414685	-7,669	1,73E-14	1,54E-11	FGE-sulfatase domain-containing protein OS=Spodoptera exigua OX=7107 GN=HW555_012305 PE=3 SV=1
TRINITY_DN2230_c0_g1_i20	O96383	780,9584	-25,8572	3,906836	-6,61846	3,63E-11	1,14E-08	Immune-related Hdd13 OS=Hyphantria cunea OX=39466 PE=2 SV=1
TRINITY_DN2230_c0_g1_i16	O96383	488,7486	-25,3283	3,906876	-6,48301	8,99E-11	2,41E-08	Immune-related Hdd13 OS=Hyphantria cunea OX=39466 PE=2 SV=1
TRINITY_DN10096_c0_g1_i12	A0A2H1VER9	276,4156	-25,2244	3,426334	-7,36193	1,81E-13	1,17E-10	SFRICE_001557 OS=Spodoptera frugiperda OX=7108 GN=SFRICE_001557 PE=4 SV=1
TRINITY_DN4227_c0_g1_i7	D0ENK2	184,8114	-24,9232	3,906918	-6,37924	1,78E-10	4,43E-08	Ornithine decarboxylase OS=Spodoptera litura OX=69820 PE=2 SV=1
TRINITY_DN7681_c0_g1_i6	A0A7E5WF69	164,8852	-24,7268	3,271552	-7,55813	4,09E-14	3,25E-11	arginine-glutamic acid dipeptide repeats protein OS=Trichoplusia ni OX=7111 GN=LOC113502148 PE=4 SV=1
TRINITY_DN1121_c0_g1_i23	A0A0N1IN40	138,0695	-24,6526	3,109138	-7,92907	2,21E-15	2,40E-12	Cleavage and polyadenylation specificity factor subunit CG7185 OS=Papilio xuthus OX=66420 GN=RR46_01469 PE=3 SV=1
TRINITY_DN3079_c0_g2_i4	A0A2H1V995	170,0287	-24,6241	3,339912	-7,37269	1,67E-13	1,10E-10	SFRICE_010949 OS=Spodoptera frugiperda OX=7108 GN=SFRICE_010949 PE=4 SV=1
TRINITY_DN2814_c0_g1_i4	A0A7E5W898	163,3298	-24,2216	3,90703	-6,19948	5,66E-10	1,26E-07	protein kinase C and casein kinase substrate in neurons protein 1-like isoform X1 OS=Trichoplusia ni OX=7111 GN=LOC113500306 PE=4 SV=1
TRINITY_DN180_c0_g1_i11	A0A7E5V8I8	117,8578	-24,1174	3,29399	-7,32164	2,45E-13	1,53E-10	uncharacterized protein LOC113491686 isoform X3 OS=Trichoplusia ni OX=7111 GN=LOC113491686 PE=4 SV=1
TRINITY_DN1782_c0_g2_i5	A0A7E5VGS4	112,978	-24,048	3,907069	-6,155	7,51E-10	1,58E-07	PAX transactivation activation domain-interacting protein OS=Trichoplusia ni OX=7111 GN=LOC113493606 PE=4 SV=1
TRINITY_DN1121_c0_g1_i18	A0A8B8HS14	117,3253	-24,0348	3,235756	-7,42789	1,10E-13	7,65E-11	cleavage and polyadenylation specificity factor subunit CG7185 isoform X4 OS=Vanessa tameamea OX=334116 GN=LOC113393619 PE=4 SV=1
TRINITY_DN350_c0_g1_i9	A0A7E5W1V3	222,1809	-23,9119	3,907106	-6,12012	9,35E-10	1,91E-07	cationic amino acid transporter 3 OS=Trichoplusia ni OX=7111 GN=LOC113498693 PE=4 SV=1
TRINITY_DN3423_c0_g1_i3	A0A2A4JVV7	102,6004	-23,7014	3,907052	-6,06631	1,31E-09	2,52E-07	Tetraspanin OS=Heliothis virescens OX=7102 GN=B5V51_10725 PE=3 SV=1
TRINITY_DN3344_c0_g1_i12	A0A2A4K1R9	86,6024	-23,6281	3,907181	-6,04734	1,47E-09	2,80E-07	PRKG1_interact domain-containing protein OS=Heliothis virescens OX=7102 GN=B5V51_6183 PE=4 SV=1

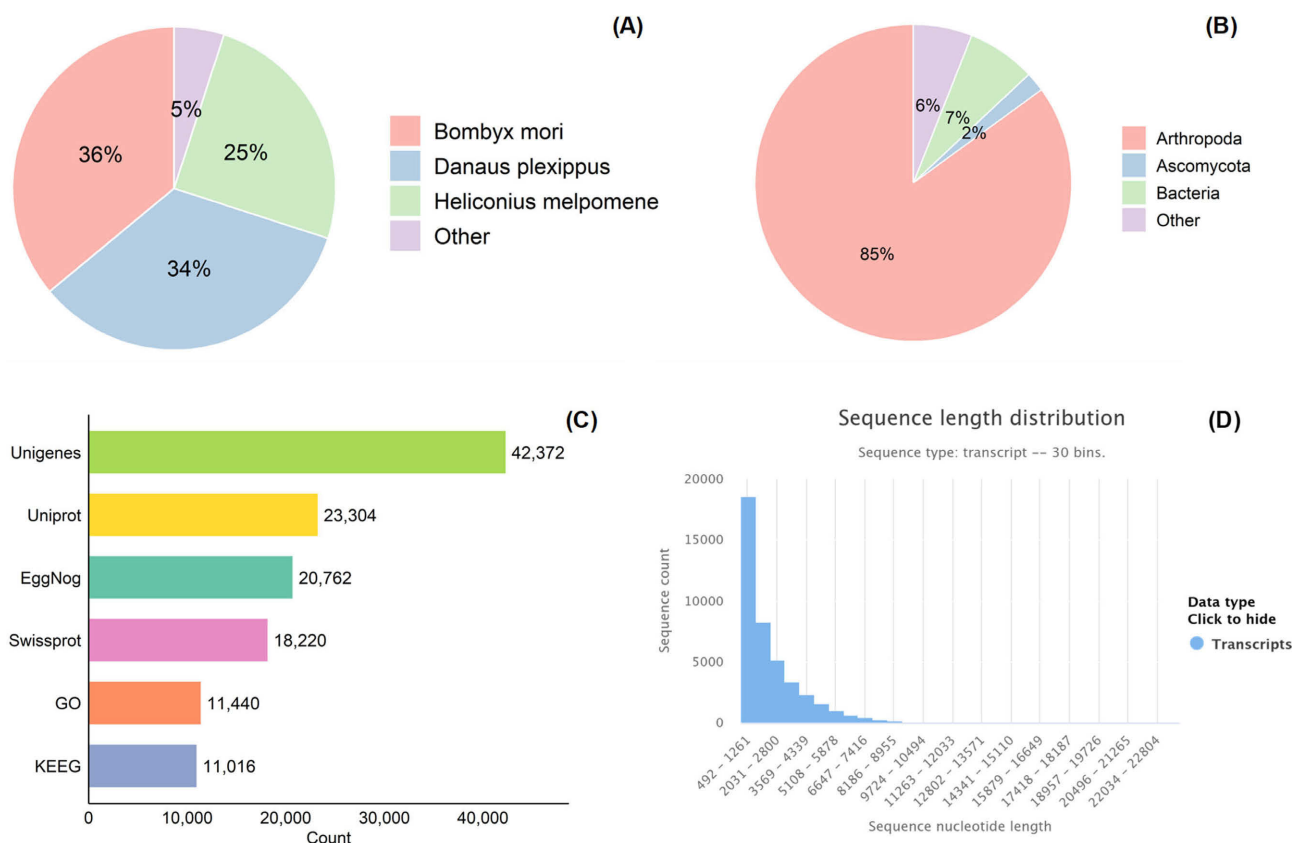


Fig. S1. Comprehensive annotation and characterization of *Anticarsia gemmatilis* midgut transcriptome based on 42,372 de novo-assembled unigenes processed through the TrapID pipeline and annotated using eggNOG-mapper v2. (A) Species-level distribution of best hits against the eggNOG 5.0 database, showing predominant similarity to *Bombyx mori* (36%), *Danaus plexippus* (34%), and *Heliconius melpomene* (25%), consistent with *Lepidopteran* proteome references. (B) Phylum-level distribution revealed a majority of transcripts affiliated with Arthropoda (85%), followed by Bacteria (7%), Ascomycota (2%), and other lineages (6%). (C) Functional annotation summary showing the number of unigenes mapped to major databases: UniProt (23,304), eggNOG orthologous groups (20,762), Swiss-Prot (18,220), Gene Ontology (11,440), and KEGG pathways (11,016), highlighting broad coverage and integration across databases. (D) Length distribution of transcripts categorized into 30 bins from 492 to 22,804 nucleotides, with a predominance of shorter contigs (≤ 1261 nt), characteristic of de novo transcriptome assemblies in non-model insects.

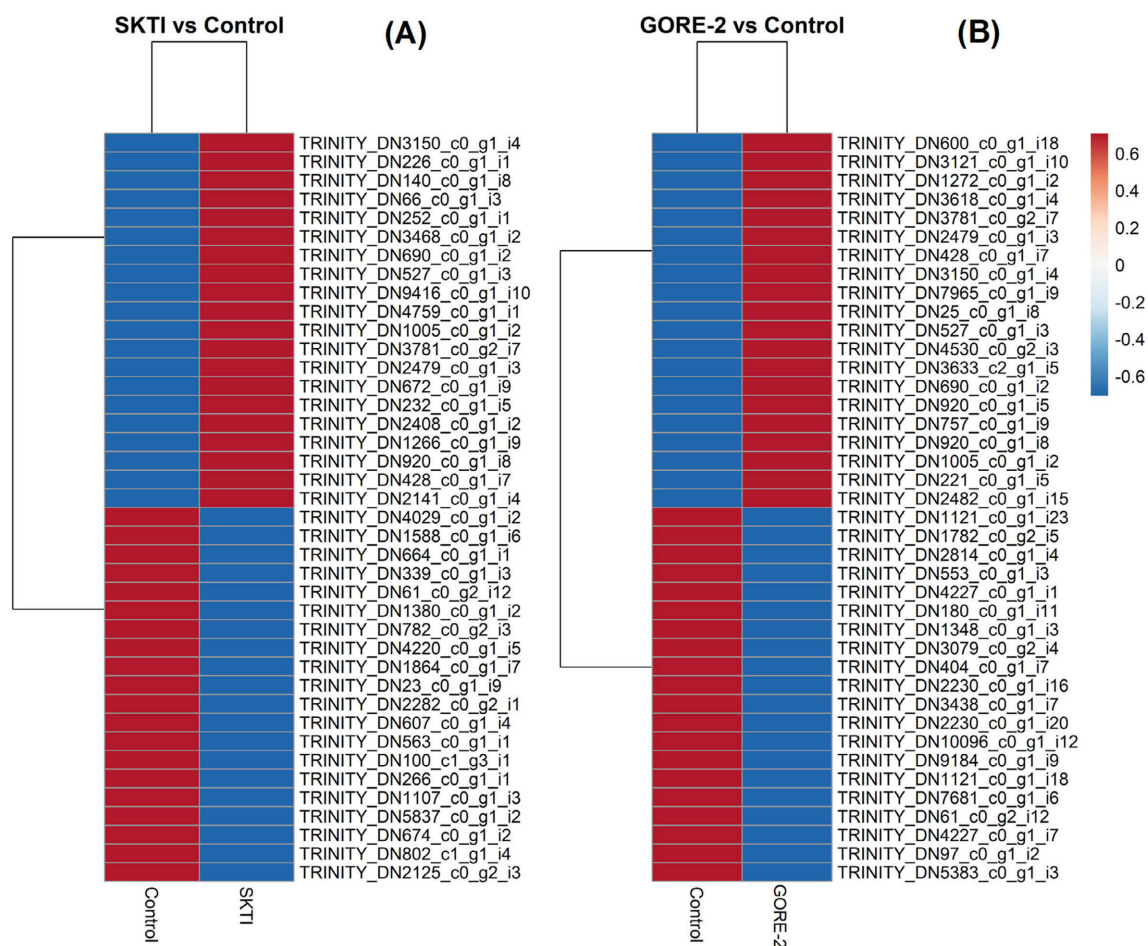


Fig. S2. Heat-map of the 20 most significant differentially expressed Unigenes in midguts of *Anticarsia gemmatalis* treated with the natural protease inhibitor SKTI and the synthetic inhibitor GORE-2 ($FDR < 0.05$, $|\log_2 FC| \geq 1$). Data depict \log_2 fold-change values normalized across samples; red indicates up-regulation and blue down-regulation relative to control. Panels are arranged as (A) Control vs SKTI and (B) Control vs VLA, highlighting inhibitor-specific expression signatures. Complete-linkage hierarchical clustering of genes (rows) and samples (columns) groups Unigenes by expression similarity, with dendrograms illustrating cluster relationships. Each row is labeled with its Trinity identifier (e.g., TRINITY_DN3150_c0_g1_i4) for precise gene tracking. Two biological replicates per condition are presented to demonstrate reproducibility. The adjacent color scale bar denotes the \log_2 fold-change values (-0.7 to $+0.7$) used in the heat-map.